BIODIESEL PRODUCTION VIA FUNCTIONALIZED GRAPHITE CATALYST

HO YEE SHEN

A project report submitted in partial fulfilment of the requirements for the award of Bachelor of Engineering (Hons.) Chemical Engineering

Lee Kong Chian Faculty of Engineering and Science
Universiti Tunku Abdul Rahman

May 2016

DECLARATION

I hereby declare that this project report is based on my original work except for citations and quotations which have been duly acknowledged. I also declare that it has not been previously and concurrently submitted for any other degree or award at UTAR or other institutions.

Signature : _____

Name : HO YEE SHEN

ID No. : 12UEB03762

Date : MAY 2016

APPROVAL FOR SUBMISSION

I certify that this project report entitled **"BIODIESEL PRODUCTION VIA FUNCTIONALIZED GRAPHITE CATALYST"** was prepared by **HO YEE SHEN** has met the required standard for submission in partial fulfilment of the requirements for the award of Bachelor of Engineering (Hons.) Chemical Engineering at Universiti Tunku Abdul Rahman.

Approved by,

Signature : _____

Supervisor : DR LEE ZHI HUA

Date : MAY 2016

Specially dedicated to

my beloved lecturers, supervisor, family and friends

ACKNOWLEDGEMENTS

I would like to take this opportunity to express my deep sense of gratitude towards the many characters that have been contributory and supportive in the successful completion of this final year project as a fractional fulfilment of the requirement for the Bachelor of Engineering (Hons.) Chemical Engineering in Universiti Tunku Abdul Rahman.

First of all, I would like to utter my utmost gratitude to my supervisor, Dr. Lee Zhi Hua for her invaluable advice and guidance throughout the development of the project. Her advices, guidance, recommendations, insights and cheerful approaches had enlightened and motivated me towards the successful completion of this project.

Furthermore, I would like to express my appreciations and thankfulness to my other partners who are Hong Wei Sam, Tan Yin Rui, Teoh Yee Ling, Wong Sin Long and Ngu Sing Yii for sharing our opinions, ideas and thoughts on various topics.

Lastly, I would also like to thank my loving parent and friends who had helped and given me constant encouragement and support, which are crucial in providing me the reason to keep striving for the best.

BIODIESEL PRODUCTION VIA FUNCTIONALIZED GRAPHITE CATALYST

ABSTRACT

In this study, the esterification process of PFAD and methanol to form biodiesel was successfully investigated using graphite as catalyst. Catalyst characterization methods such as XRD, SEM and FTIR were completed on the graphite catalysts based on different preparation conditions. The three types of catalyst investigated were original, purified and sulfonated graphite catalysts. Besides that, GC was carried to determine the yield of biodiesel for different process parameters such as methanol-to-PFAD ratio, reaction temperature and catalyst loading. From the XRD analysis, sulfonated graphite catalyst has smaller crystallite sizes and greater integrity intensity. For SEM spectroscopy, sulfonated graphite catalyst has more defects and cracks, which contribute to greater number of active sites. For FTIR spectroscopy, the presence of sulfonate groups, O=S=O stretching vibrations and S-O groups was only shown in the sulfonated graphite catalyst but not the others. It indicated the practicality of introducing SO_3H groups on the surfaces of graphite catalyst through sulfonation. For GC analysis, some process parameters such as were selected to investigate their effect on the biodiesel yield and to predict their optimal values. The optimal methanol-to-PFAD ratio, reaction temperature and catalyst loading were 30.0, 170 ℃ and 3 wt%, respectively. These results were tally with the one suggested by using software DesignExpert8 where it was more preferable to have high temperature and high catalyst loading since it offered a more accurate analysis.

TABLE OF CONTENTS

LIST OF TABLES

LIST OF FIGURES

LIST OF SYMBOLS / ABBREVIATIONS

n	number of order
d	lattice plane distance
T_m	peak maximum temperature, K
λ	wavelength, m
θ	diffraction angle, °
τ	crystallite size, m
ASTM	American Standards for Testing Materials
ATR	attenuated total reflectance
BET	Brunauer-Emmett-Teller
CaO	calcium oxide
CH_3OH	methanol
CH_3SO_3H	methanesulfonic acid
$(CH_3CO)_2O$	acetic anhydride
CNT	carbon nanotube
CO	carbon monoxide
DW	distilled water
EDX	Energy Dispersive X-Ray
EN	European Union
Et_3N-CNT	amino-functionalized carbon nanotube
FAME	fatty acid methyl ester
FFA	free fatty acid
FID	flame ionization detector
FT-IR	Fourier Transform-Infrared
FWHM	full width at half maximum
GC	gas chromatography

HCl	hydrochloric acid
HI	hydrogen iodide
HNO_3	nitric acid
H_2SO_4	sulfuric acid
ICP-MS	inductively coupled plasma mass spectrometry
IEA	International Energy Agency
JCPDS	Joint Committee Powder Diffraction Standard
KOH	potassium hydroxide
MWCNT	multi-walled carbon nanotube
NaOH	sodium hydroxide
PFAD	palm fatty acid distillate
Pt	platinum
PXRD	powder X-ray diffraction
SEM	Scanning Electron Microscope
SEM-EDX	Scanning Electron Microscopy with Energy Dispersive X-Ray
TCD	thermal conductivity detector
TGA	Thermal Gravimetric Analysis
TEM	Transmission Electron Microscope
TPD	Temperature Programmed Desorption
XRD	X-ray diffraction
ZnO	zinc oxide

LIST OF APPENDICES

CHAPTER 1

INTRODUCTION

1.1 Renewable Energy Sources

Energy and environment are two major concerns around the world. Extensive use of natural gas, crude oil and coal has resulted in climate change and increasing prices for energy (Rexhäuser and Löschel, 2015). According to Lam et al. (2010), there is a serious need to look for more renewables to keep up with future demand and sustain energy security worldwide. Having said that, the world is still heavily dependent on fossil fuels with the expected share in global energy at about 75 % in 2035 (IEA, 2014). Even though oil will remain as the major energy source, the oil share was forecasted to drop from 35 % in 2007 to 30 % in 2035 in the world marketed energy consumption as shown in Figure 1.1 (Atabani et al., 2012).

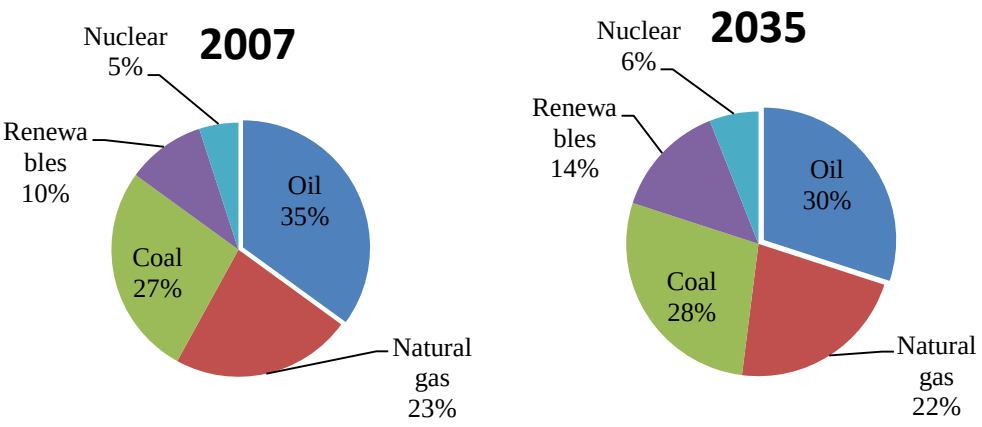

Figure 1.1: Comparison of energy consumption in 2007 with 2035 (Atabani et al., 2012).

Renewable energy, in the past ten years, has been recognized to have the potential to replace the conventional fossil fuels. Besides, renewable energy sources have been utilized successfully to reduce the dependency of fossil fuels. According to a study constructed from International Energy Agency (EIA), the energy source with the highest potential among other renewable energies is the energy produced from renewables and wastes (Lam et al., 2010).

Among the renewable energies, considerable focuses and attentions have been given on biodiesel due to its high availability of inexhaustible feedstock. In 1893, peanut oil was used by Rudolf Diesel for his engine as transportation fuel for the first time (Zabeti et al., 2009b). Biodiesel was then brought into South Africa to power vehicles. Vegetable oils were already used as fuels during 1930s and 1940s. In 1982, an active discussion on these as fuels was held in an international conference in Fargo, North Dakota (Ma and Hanna, 1999).

1.2 Background of Biodiesel

Biodiesel is a substitute diesel fuel derived from biological substances such as animal fats and vegetable oils. Triglycerides, consisting of different fatty acid chains, are the major constituents of these oils and fats. Different fatty acid chains will have different physicochemical properties and their compositions will be of paramount importance because they will affect the properties of the biodiesel produced (Lam et al., 2010).

The direct use of oils and fats as fuels is restricted because of their high kinematic viscosity and low volatility. In addition, they would cause serious complications such as carbon deposition and ring sticking in the engine. Thus, they must be subjected to transesterification to convert triglycerides into fatty acid methyl ester (FAME) (Lam et al., 2010). According to ASTM D6751, a standard biodiesel should have a minimum ester content of 96.4 % (Jakeria et al., 2014).

Figure 1.2 depicts the transesterification reaction between triglyceride and methanol to form FAME and glycerol (Lam et al., 2010).

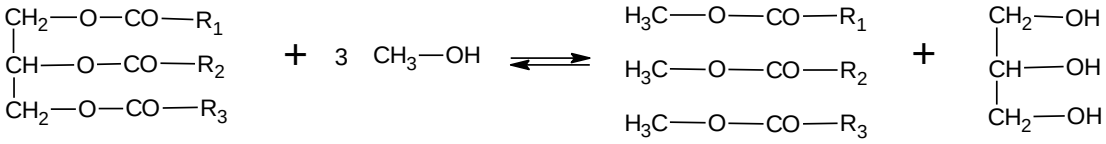

Figure 1.2: Transesterification reaction (Lam et al., 2010).

1.2.1 Properties of Biodiesel

The improvements on the quality of biodiesel are being developed on a global scale to assure that a high-quality biodiesel is made available to the consumer. Due to the varying origins and qualities of biodiesel produced from differently scaled plants, it is essential to adhere to a standard of fuel quality to ensure good engine performance (Atabani et al., 2012).

Currently, international standard specifications of biodiesel must be adhered to in order to ensure the acceptable biodiesel properties and qualities. These specifications include the European Union (EN 14214) Standards and the American Standards for Testing Materials (ASTM 6751 for biodiesel fuel. The main properties of petroleum diesel and biodiesel are shown in Table 1.1 (Atabani et al., 2012).

Table 1.1: Comparison on the main properties of diesel and biodiesel (Atabani et al., 2012).

Fuel properties	**Diesel Fuel**	**Biodiesel**	
	ASTM D975	**ASTM D6751**	**DIN 14214**
Density at 15 ℃ (kg/m^3)	860	890	870-910
Viscosity at 40 ℃	2.60	1.90-6.00	3.50-5.00
Acid value (mg KOH/g)	0.06	≤0.50	≤0.50
Flash point	60.0-80.0	100-170	>120
Oxidation stability (hour)	-	3 min	6min

1.2.2 Advantages of Biodiesel

One of the advantages of biodiesel is that it can reduce the carbon dioxide emissions by 78 % compared to conventional diesel fuel while having high combustion characteristics (Liaw, 2013). Since biodiesel is renewable, non-flammable, non-toxic, readily available, biodegradable, portable, eco-friendly, sustainable, sulfur-free and free from the hazardous aromatic compounds, it becomes an ideal choice of fuel for heavily polluted cities. Moreover, biodiesel reduces the amount of particulate matter in ambient air and thus, reducing air toxicity (Atabani et al., 2012). In addition, biodiesel production is less time-consuming and can be raised easily since it does not involve upstream processes such as drilling, transportation and refining as that of petroleum diesel (Atabani et al., 2012). Figure 1.3 shows that the annual production of biodiesel has increased from 15 thousand barrel per day in 2000 to 289 thousand barrel per day in 2008 (Atabani et al., 2012).

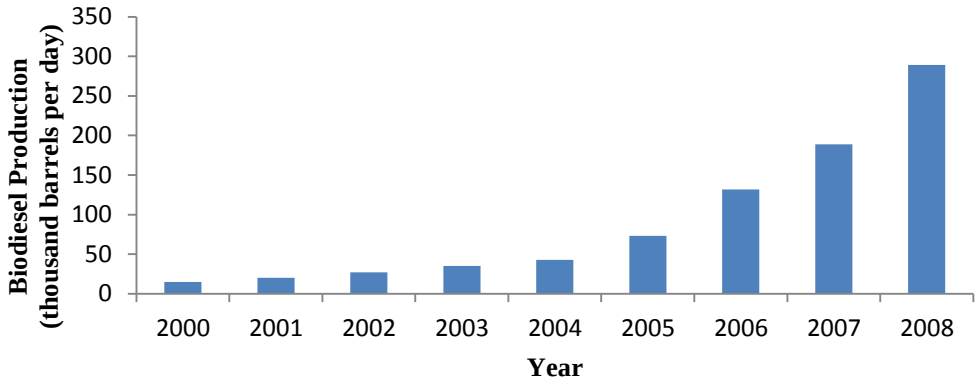

Figure 1.3: Total world biodiesel productions between 2000 and 2008 (Atabani et al., 2012).

Furthermore, biodiesel has incredible lubricating properties. This enhances lubrication in injector units and fuel pumps, which will reduce wear and tear while increasing engine efficiency. Not only that, biodiesel is harmless for transportation handling, distribution, storage and utilization because of its higher flash point than

that of petroleum diesel. Lastly, biodiesel has greater cetane number and this decreases the ignition delay (Tay, 2012).

1.2.3 Disadvantages of Biodiesel

Even though biodiesel offers a number of advantages, there are still some limitations in using biodiesel as fuel oil. First of all, biodiesel consumes more fuel (about 2-10 %) than diesel because it has lower energy content than diesel. Besides, due to its lower volatilities, it which lead carbon deposition and gum formation due to incomplete combustion (Tay, 2012). This will cause contamination of oil and suffer from flow problem. In addition, due to its higher viscosity and lower volatility, higher injector pressure is required (Atabani et al., 2012).

Moreover, biodiesel has lower oxidation stability than that of petroleum diesel. This means that biodiesel can be oxidized easily into fatty acids in the presence of air, leading to corrosion of pipe, injector and fuel tank. Lastly, transesterification process causes a number of environmental problems such as soap formation, disposal of wastes and water requirement for washing (Atabani et al., 2012).

1.3 Problem Statement

Edible oils like rapeseed, coconut, palm, canola, corn, and peanut are commonly used to produce biodiesel. Currently, edible oils accounts for more than 95 % of the world biodiesel (Atabani et al., 2012). Nevertheless, the using of edible oils creates some hurdles to the further development of biodiesel. One of the major problems is that it raises concerns on the food versus fuel issue (Shuit and Tan, 2014). Various organizations have raised objections towards this practice, complaining that biodiesel is rivalling resources with the food industry (Shuit et al., 2010). Besides, it creates

many environmental implications such as deforestation, soil destruction and use of many lands for agricultural purposes. In addition, the price of refined vegetable oils is unstable and fluctuating. In the past years, the values of vegetable oil plants have skyrocketed and this will affect the biodiesel industry in terms of economic viability. Not only that, the using of edible oils to produce biodiesel is not practical in the long-run due to the rising gap between supply and demand of those oils in many countries (Atabani et al., 2012).

The use of conventional heterogeneous catalysts creates some limitations such as mass transfer limitation, low reusability and stability of the catalyst, and high costs of catalysts. These limitations will be reviewed further in the following section.

1.3.1 Limitations of Conventional Heterogeneous Catalysts

1.3.1.1 Mass Transfer Limitation

Conventional heterogeneous transesterification reactions commonly have limitations on the mass transfer resistance owing to the presence of triglyceride, methanol and catalyst. The main reason is that the available diffusion process of pores and the active sites are limited. This will in turn decreasing the rate of esterification reaction (Mbaraka and Shanks, 2006). According to Lee and Saka (2010), co-solvent can be used to overcome the mass transfer limitation by increasing the oil to alcohol miscibility, and improving the interaction between reactants and solid catalysts. However, the presence of co-solvent can cause glycerol adhesion on the catalyst particle which in turn deactivates the catalyst. This will also increases the overall processing steps and consumption of energy due to the extra separation process.

Meanwhile, the mass transfer problem can be addressed through the application of catalyst supports. This is because they have high specific surface areas and are highly porous for the active phase to anchor. This will enhance the contact between the triglycerides or fatty acid molecules and the catalyst (Shuit et al., 2013).

According to Zabeti et al. (2009a), it is reported that all supports with high thermal and chemical stability can be utilized as catalyst supports. Examples of the most common support materials used for either transesterification or esterification are alumina, silica, activated carbon, zeolite, carbon nanotubes (CNT) and even graphite.

1.3.1.2 Low Reusability and Stability of the Catalyst

Low reusability and stability are two main concerns that have to be taken into account when using heterogeneous catalyst for biodiesel production (Lee and Saka, 2010). According to Alonso et al. (2007), the main factors of catalysts deactivation are deposition of organic substances on the catalyst surface and leaching of the active species. Even though calcium oxide (CaO) is frequently used in producing biodiesel, significant amount of CaO leached was detected during transesterification reaction (Kouzu et al., 2009). It was stated by Kouzu et al. (2009) 10.5 wt% of CaO has leached away during the first set of the transesterification, decreasing the yield of biodiesel.

Apart from that, one more reason is the adsorption or deposition of organic substances, particularly carbon onto the surface of catalyst (Shuit et al., 2013). According to Ngamcharussrivichai et al. (2008), it was described that over 12 wt% of organic substances was deposited on the CaO-ZnO catalyst used in transesterification reaction of the palm kernel oil.

1.3.1.3 High Cost and Non-renewable Nature of Catalysts

Another major disadvantage of using conventional metal type heterogeneous catalysts in biodiesel production is their high costs and non-renewable nature (Mo et al., 2008). Compared to the homogeneous catalyst, most of the metal catalysts are more expensive (Lee and Saka, 2010). Zong et al. (2007) reported that expensive

metal catalysts have given satisfying catalytic activity and stability during the simultaneous esterification and transesterification of oils with high free fatty acid (FFA) content. However, they have not been widely applied in the industry mainly due to their rareness and costs.

1.4 Aims and Objectives

The objectives of the project are listed as follows:

I. To prepare graphite catalyst through sulfonation for the esterification reaction of PFAD with methanol.
II. To study and optimize the effect of process parameters, namely reaction temperature, methanol-to-PFAD ratio and catalyst loading in the esterification of PFAD, using functionalized graphite catalyst.
III. To characterize the functionalized graphite catalyst.

1.5 Scope of Study

The scope of this research study was limited to the esterification reactions based on different biodiesel synthesis technologies, various catalysts used for biodiesel synthesis, background and preparation of the proposed catalyst, assessment on different process parameters, and some characterization methods. Where necessary, non-esterification related works, such as those relating to transesterification, are reviewed as well so that the researcher and reader are more understand and familiar with this study.

1.6 Outline of Thesis

Chapter 1 (Introduction) will mainly cover the brief background and review of the biodiesel, problem statement, and objectives.

Chapter 2 (Literature Review) will mainly cover the PFAD as feedstock, transesterification and esterification, catalysis in esterification, catalyst support, and process parameters that affect the biodiesel synthesis.

Chapter 3 (Materials and Methods) will mainly cover the types of materials used, catalyst preparation, esterification conditions, FAME analysis and different characterization methods.

Chapter 4 (Results and Discussion) will mainly cover the determination and discussion of the optimum conditions for biodiesel synthesis based on the process parameters tested.

Chapter 5 (Conclusion and Recommendations) will mainly cover the general conclusion established from this study and recommendations will be suggested.

CHAPTER 2

LITERATURE REVIEW

2.1 PFAD as Feedstock

There is a wide range of feedstocks available for the biodiesel production, ranging from edible oils, non-edible oils, waste oils and animal fats. Figure 2.1 shows that the feedstock alone represents 75 % of the overall production cost of biodiesel (Atabani et al., 2012).

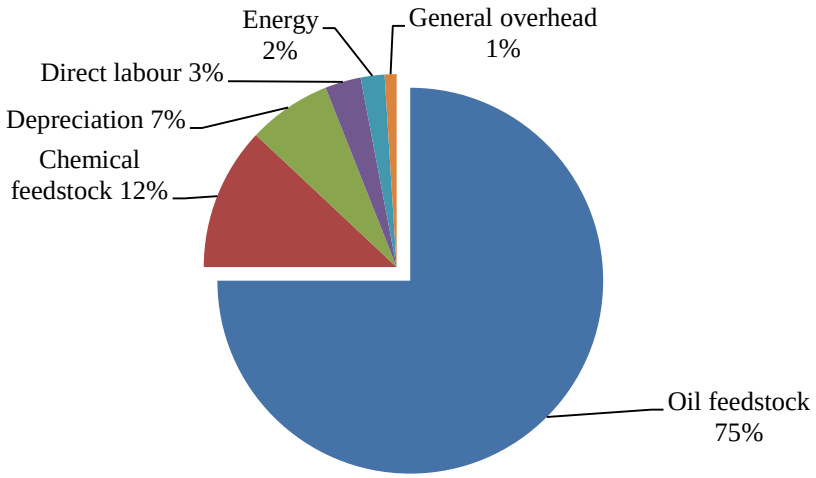

Figure 2.1: General cost breakdown for biodiesel production (Atabani et al., 2012).

Biodiesel is usually produced using refined edible oils such as soybean, sunflower oil and so on. However, this practice causes the price of refined vegetable oils to be fluctuating and eventually biodiesel production will not be economically feasible (Shuit and Tan, 2014).

Therefore, non-edible oils such jojoba, rubber seed and PFAD are now gaining attention because they seem to be a promising substitute for biodiesel production. Among the non-edible oils, PFAD appear to be the most promising and is the most suitable for Malaysia scenario (Shuit and Tan, 2015). This is because PFAD is a low-value, non-food by-product generated in the fatty acid stripping and deodorization stages during the refining of palm oil (Olutoye et al., 2014). Besides, PFAD refinery costs is much cheaper (only 0.37 USD per litre) than that of other refined vegetable oils (Yujaroen et al., 2009). In addition, the high miscibility of FFA of PFAD in methanol reduces the mass transfer limitation instigated by immiscibility between methanol and oil (Shuit and Tan, 2014). According to Chongkhong et al. (2007), PFAD has high FFA content of about 93 wt%.

2.2 Transesterification and Esterification

Globally, sufficient amount of efforts are required to develop and improve the production of biodiesel. Common limitations linked with the usage of crude vegetable oils are their high viscosities, low relative volatilities and their polyunsaturated characters. Hence, there are four common technologies used to overcome these issues which are pyrolysis, dilution, micro-emulsion and transesterification/ esterification (Atabani et al., 2012). Among the four methods, transesterification/ esterification is the most popular and widely used method (Tay, 2012). Transesterification and esterification reactions are closely related to each other since they are can be carried out separately or simultaneously in one-step or two-step reaction, respectively (Atadashi et al., 2012).

2.2.1 Transesterification

Transesterification involves a series of consecutive and reversible reactions (Atabani et al., 2012). First step is where the triglycerides is converted to diglycerides, followed by the second step where diglycerides is converted to monoglycerides, and finally the conversion of monoglycerides to glycerol (Shuit et al., 2013). One FAME molecule will be produced from each individual steps (Abbaszaadeh et al., 2012). The transesterification reaction of triglyceride is illustrated in the following equations (Atabani et al., 2012).

$$\text{Triglyceride} + \text{ROH} \leftrightarrow \text{Diglyceride} + \text{FAME} \quad (2.1)$$

$$\text{Diglyceride} + \text{ROH} \leftrightarrow \text{Monoglyceride} + \text{FAME} \quad (2.2)$$

$$\text{Monoglyceride} + \text{ROH} \leftrightarrow \text{Glycerol} + \text{FAME} \quad (2.3)$$

Hence, the overall reaction is

$$\text{Triglyceride} + 3\,\text{ROH} \leftrightarrow 3\,\text{FAME} + \text{Glycerol} \quad (2.4)$$

The glycerol produced will sink to the bottom and the biodiesel which floats on top will then be siphoned out. The common alcohols used are methanol and ethanol due to their fairly low cost. Nevertheless, other alcohols such as propanol, butanol, branched alcohol, isopropanol and so on can also be used but they are of higher cost (Atabani et al., 2012).

For each transesterification reaction, three moles of alcohol will react with one mole of vegetable oil to form three moles of FAME and a glycerol (Liaw, 2013). Since alcohol is less soluble in either oil or fat, the use of a homogeneous catalyst is commendable to commence the reaction. This is because the homogeneous catalyst improves the miscibility of alcohol in the reaction mixture and thus, increasing the rate of reaction (Atabani et al., 2012). The most common catalyst for transesterification is homogeneous basic catalysts such as KOH and NaOH.

2.2.2 Esterification

Esterification is a chemical reaction between FFA and alcohol (usually methanol) to form alkyl ester and water (Zhang et al., 2003). Esterification of FFA takes place much more rapidly than transesterification of triglycerides. The reason for this is that esterification is a one-step reaction while transesterification is a three-step consecutive reaction (Warabi et al., 2004). The intermediate steps of removing the fatty acid chains from the glycerine backbone are not present. Therefore, water is the by-product and not glycerol (Altic, 2010).

$$RCOOH + CH_3OH \leftrightarrow RCOOCH_3 + H_2O \quad (2.5)$$

The esterification reaction between fatty acid and methanol to form FAME and water is depicted in the chemical equation above (Liaw, 2013). Acid catalyst is generally used to catalyze the esterification reaction. This is because fatty acids will react chemically with the basic catalysts such as NaOH and KOH to form soap by saponification. According to Tyson (2005), the FFA mass concentrations above 4 % will produce more soap in a conventional base-catalyzed reaction which will cause incomplete reactions to take place. Besides, Islam et al. (2014) stated that the alkali catalyzed reaction gives a lower biodiesel yield for low grade feedstocks with high FFA content because the soap formation resulted serious emulsification and separation problems. These studies clearly imply that the conventional method of biodiesel synthesis using basic catalyst is ineffective for oils with high FFA content.

Thus, esterification would be a sounder option than transesterification for non-edible oils with high content of FFA. Since PFAD contains high amount of FFA (93 wt%), esterification is selected to be the reaction to produce biodiesel.

2.3 Catalysis in Esterification

Esterification can be carried with or without catalyst. The main focus in this study was to produce biodiesel using acid catalyst. Acidic catalysts in esterification composed of homogeneous catalyst and heterogeneous catalyst.

2.3.1 Homogeneous Acidic Catalyst

The most common homogeneous acidic catalysts for esterification are sulfuric acid (H_2SO_4) and hydrochloric acid (HCl). Warabi et al. (2004), concluded that H_2SO_4 and methanesulfonic acid (CH_3SO_3H) are two of the best catalysts. These catalysts give high conversion of 90 % biodiesel. Besides, these homogeneous acid catalysts can convert feedstock with high FFA into biodiesel with yield that higher than 90%. This is because homogeneous acidic catalyst can catalyze both esterification and transesterification to convert the FFA and triglycerides into fatty acid methyl ester without any soap.

However, the disadvantages of using homogeneous acidic catalyst are the formation of acid effluent, catalyst non-reusability and high equipment costs. Moreover, it has low catalytic activity due to longer reaction time and requires high mole ratio of methanol to oil required (Wang et al., 2006). Referring to a study conducted by Melero et al. (2015), it was found that the usage of H_2SO_4 as homogeneous acidic catalyst led to biodiesel production with high sulfur content and thus, the international specification cannot be met and the produced biodiesel is required to be further processed to reduce the sulfur content.

2.3.2 Heterogeneous Acidic Catalyst

Some of the common heterogeneous acidic catalysts include ion-exchange resin, sulfated oxides, and sulfated carbon based catalysts. Heterogeneous acid catalyst can

eliminate the problem of equipment corrosion and the treatment of water effluent produced after the process by using homogeneous acidic catalyst (Shu et al., 2010). Besides, heterogeneous acidic catalysts can be removed easily from the reaction medium through filtration and the catalyst can be recycled and reused in the new process. In short, it gives better separation with less catalyst lost (Melero et al., 2010). Not only that, the usage of heterogeneous acid catalyst offers higher stability, which means better tolerance for FFA without catalyst deactivation (López et al., 2005)

Although heterogeneous acid catalyst seems to offer quite a number of advantages, it has its drawbacks as well. According to López et al. (2005), heterogeneously catalyzed reaction has low catalytic activity. Some other groups of author also stated that heterogeneous catalyzed reaction requires extreme reaction conditions to increase the biodiesel yield and to cut down the reaction time (Rattanaphra et al., 2012).

2.4 Catalyst Support

The mass transfer limitation can be considerably lowered through the use of a catalyst support. The reason is that it provides higher external surface area (Pham Huu et al., 1987). A catalyst support with presence of pores where active components can be attached on provides higher surface area. For most of the solid catalyst, active component and support are the two major components involved. A particular support is chosen based on the reaction conditions and the nature of application. The support properties are mainly affected by the preparation procedures and the quality of the materials used (Islam et al., 2014).

Commonly, it is necessary for heterogeneous catalysts to be microporous or mesoporous for easy separation from the fluid reactants and products. Due to their nano-sized characteristics, agglomeration of heterogeneous catalysts is a common phenomenon. Catalyst support provides high specific surface area for the strong attachment of nano-sized heterogeneous catalysts and to reduce the agglomeration of heterogeneous catalyst (Julkapli and Bagheri, 2015).

In addition, high dispersion of active site phase on the surface can be achieved by using catalyst support. It is clear that the higher the surface area formed by pores which can be accessed, the higher the dispersion of active catalyst (DeCastro et al., 2000).

2.4.1 Carbon Materials as Catalyst Support

Nanomaterials made up of carbon have always been utilized as support medium owing to its remarkable tensile strength, thermal stability, high surface area, and recyclability. This is essential in keeping up with the sustainable chemistry protocol (Wu et al., 2011). According to Wang et al. (2007), surface functionalization was suggested to be one of the possible routes to improve the support properties of carbon materials.

The key leading to noteworthy selectivity and cost reduction of catalyst is the blend of nanocarbon materials and heterogeneous catalysis (Ioroi et al., 2006). The activity and selectivity of a catalyst supported on carbon-based catalyst support largely depends on the atomic structure of its active site (Shen et al., 2014). Meanwhile, the active sites depend on the porosity of the catalyst support, varying in size from nanometres to centimetres (Gong et al., 2014). Therefore, by distributing the active sites microscopically, the availability of the active site in carbon-based catalyst support can be enhanced (Chekin et al., 2013).

The physical and chemical properties of the support surface can be designed to create a large specific surface area for large scattering of the active phase (Mosaddegh and Hassankhani, 2014). Lastly, the presence of carbon support materials can encourage some interactions between active phase and support which further increase the catalyst stability and reusability (Jing et al., 2014).

2.4.2 Desirable Properties of a Catalyst Support

Figure 2.2 shows the deposition of catalyst on both porous and non-porous support. It is obvious that the porous catalyst support offers a greater specific surface area which leads to greater dispersion of the catalysts.

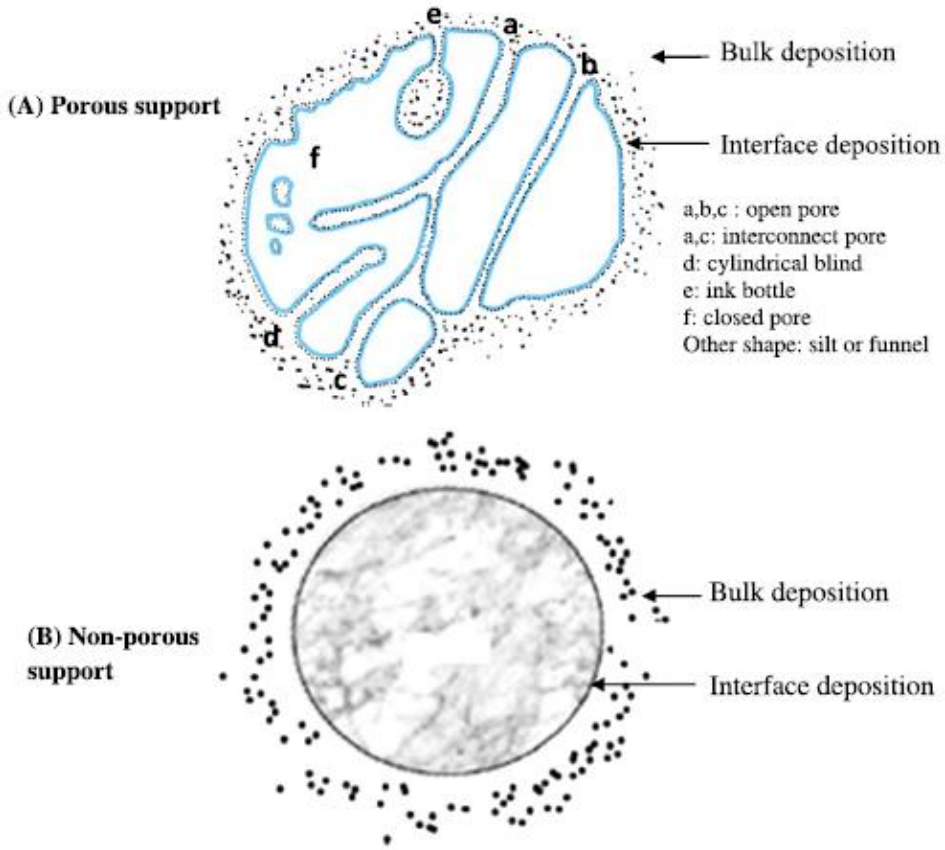

Figure 2.2: Catalytic particles supported on porous and non-porous supports (Islam et al., 2014).

Much attention has been given in recent years on the modification of support microstructure due to the unique properties (Borges and Díaz, 2012). Based on the survey done on different studies, few vital properties of the catalyst support are listed as follows:

- Inertness. Catalyst support should not involve in the catalytic reaction which may lead to undesirable side reactions (Perego and Villa, 1997).

- Stability. Support materials involved in reaction and regeneration should possess high chemical and thermal stability (Chuah et al., 2000).
- Shape. The shape of support materials are preferred to be spherical to minimize resistance caused by the collision with reactants and products (Islam et al., 2013)
- Porosity. The active components are usually dispersed on the surface of a porous or non-porous support as shown in Figure 2-2 (Islam et al., 2014).
- Size. The activity of the catalyst depends on the particle size. The smaller the particle, the greater the specific surface area and thus, the higher the rate of reaction (Kuila et al., 2014).
- High surface area and desirable mechanical strength (Kuila et al., 2014).
- Low cost (Islam et al., 2014).

2.5 Functionalized Graphite as the Proposed Catalyst for Esterification

The application of graphite as catalyst support in biodiesel production still remains unexplored. Therefore, more studies are required to provide significant insights for graphite-supported heterogeneous acidic catalysts.

2.5.1 Properties, Characteristics and Applications of Graphite

Graphite is a crystalline and highly ordered material composed of aromatic sheets with a constant interlayer spacing of 0.335 nm. Graphite is generally non-porous and has a low active surface area (10 m^2/g). However, atoms and smaller molecules can slip between layers, providing a confinement effect (d'Halluin et al., 2015).

Apart from that, graphite is chemically inert to acid and alkali under most conditions. Besides, it also has high thermal stability up to 3200 ℃ under vacuum or inert atmospheres. However, it oxidizes at about 400 ℃. Unlike diamond, graphite is

an electrical conductor and it is usually used in electrodes. Moreover, graphite is also applied as a structural material due to its remarkable strength to weight ratio and it is of low cost (Dimovski, 2006). Figure 2.3 shows the basic structural unit of disordered graphite (Dimovski, 2006).

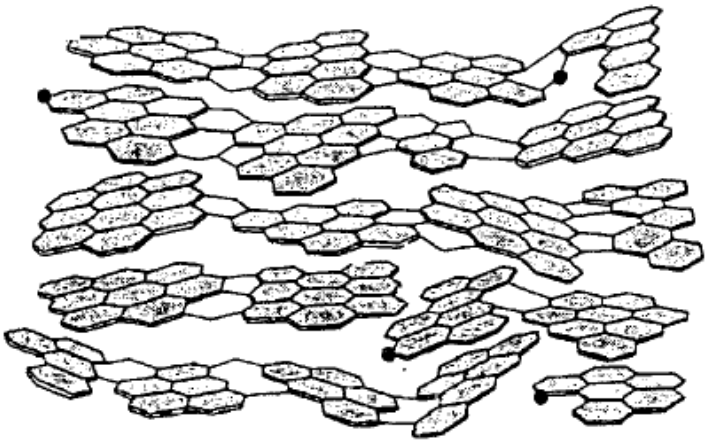

Figure 2.3: Basic structural unit of disordered graphite (Dimovski, 2006).

In graphite, every carbon atom is bonded covalently to three other carbon atoms with short (1.418 Å) and strong (524 kJ/mole) sigma bonds in hexagonal pattern. All the sigma bonds belong to a single plane, known as a basal plane. This sp^2 bonded carbon atoms is called a graphene layer when isolated. Graphene sheets are formed from pure sp^2 carbon while the three-dimensional (3D) bonding network of sp^3 carbon can only be found in diamond (Dimovski, 2006). When a planar graphene sheet is folded as in fullerenes and carbon nanotubes, there is a partial loss of sp^2 hybridization and increase in the sp^3 character due to the change in bond angles (Dimovski, 2006).

2.5.2 Utilization of Graphite as Catalyst Support in Other Studies

Figure 2.4 depicts the morphology of the graphite support (G) and cobalt boride catalysts supported on the graphite support (Co-B/G). From the figure, it can be observed that graphite is made up of planar sheets with different thickness. For the

graphite supported cobalt boride catalysts, the fibrous cobalt boride of different sizes are deposited on the graphite support (Özdemir, 2015).

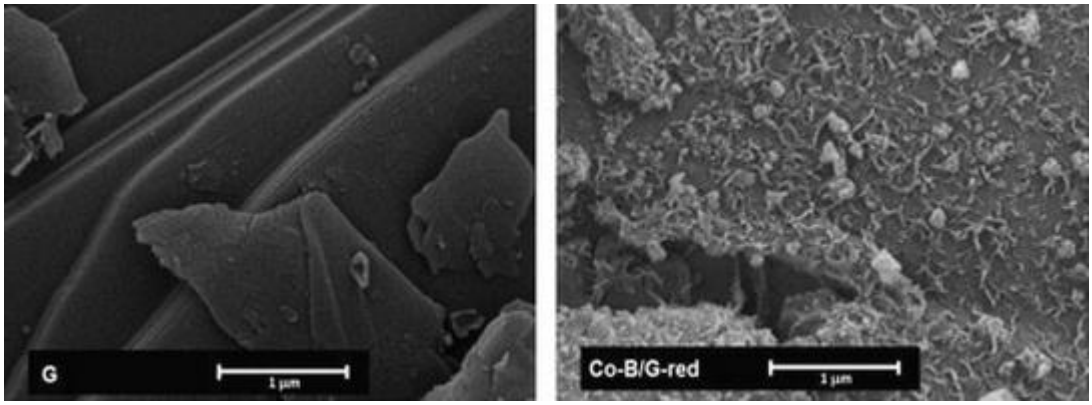

Figure 2.4: SEM images of the carbon supports and catalysts (Özdemir, 2015).

Özdemir (2015), evaluated the catalytic activity of cobalt boride catalysts supported on graphitic and amorphous carbon derivatives, namely graphite and glassy carbon. The goal of the study was to reveal the influence of catalyst preparation route on $NaBH_4$ hydrolysis rate for cobalt catalyst supported on graphite and glassy carbon. The size of the graphite used was reported to be less than 20 μm. By using powder X-ray diffraction (PXRD), the peaks for graphite were centered at 26.54° and 54.63° scattering from the 002 and 004 planes of graphite. The results of the study showed that Co-B/graphite enhanced the volume of hydrogen evolution.

Ramos-Sánchez and Balbuena (2014), studied on the adsorption of carbon monoxide (CO) on platinum (Pt) clusters supported on graphite. The adsorption energies were evaluated on different sites of Pt clusters supported on graphite. In the study, the graphite was reported to have the capacity to accept electrons from the deposited clusters and will exchange donate electrons when the Pt clusters absorbs CO.

Wang et al. (2013), studied on the comparisons of Pt catalysts supported on AC, carbon molecular sieve, CNTs and graphite for hydrogen iodide (HI) decomposition at varying temperature. The catalytic performances on the HI decomposition were assessed at a temperature range of 400 to 500 ℃ under

atmospheric pressure. The graphite supported catalyst showed good activity at higher temperatures

d'Halluin et al. (2015), evaluated the preparation, characterization and catalysis applications of graphite-supported ultra-small copper nanoparticles. The ultra-small copper nanoparticles were reported to be well spread onto the graphite support and yield very narrow distribution in size, which is in the range from 1.6 to 2.6 nm. This heterogeneous catalyst was successfully evaluated and the catalyst was easily recovered by filtration, leaving the crude mixture virtually free of copper residues, as evidenced by ICP-MS analyses.

2.5.3 Advantages of Graphite in Other Conventional Catalysts

The limitations of the conventional heterogeneous catalysts such as low stability, mass transfer problem, high cost of catalyst and limited reusability can be improved by using graphite as catalyst support. Functionalized graphite is deemed to have the capability to be the ensuring catalyst for use in the production of biodiesel. As mentioned previously, the intrinsic properties of graphite are highly crystallized, highly ordered, chemically inert, high thermal stability, high strength to weight ratio, and low cost. The advantages and desirable properties of in biodiesel synthesis will be reviewed in the next session.

2.5.3.1 Excellent Catalyst Stability

Conventional catalysts are commonly prepared by precipitation methods. Carbon materials, such as CNT can be tailored to be catalytically energetic through functionalization with specific functional groups onto its surface (Balasubramanian and Burghard, 2005). Besides, leaching of active sites was reported to have occurred under liquid-phase reactions because they are not covalently bonded to the solid catalyst support (Li et al., 2011). CNTs seem to be the perfect choice of support for

biodiesel production. The reason is that the active sites or functional groups are covalently bonded to CNTs (Balasubramanian and Burghard, 2005). So, the leaching of the active phase into the reaction mixture is less likely to occur because the strong covalent bonds will not simply broken under reaction temperature (Salavati-Niasari et al., 2008).

Since graphite and CNT are both comprised of a network of carbon atoms, it is most likely that the graphite would act the same way and possess the same properties as that of CNTs. Meanwhile, the covalent bonding offers good stability, accessibility and selectivity. Hence, graphite would be an appropriate alternative to overcome the low stability problem.

2.5.3.2 Low Catalyst Cost

As mentioned, one of the major hindrances in using metal catalysts for producing biodiesel is their high catalyst cost. Even though the production cost for graphite is still high at this moment because it is still in research stages, graphite has a huge potential to be in mass scale production with lower production cost. Therefore, replacing valuable metal catalysts with functionalized graphite as supporting materials in esterification is more economically feasible since the cost for graphite is low. Besides, unlike other precious metal, graphite is more renewable because it can be regenerated by using methane (Özdemir, 2015).

2.6 Process Parameters that Affect Biodiesel Synthesis

In order to synthesize sustainable and cost-effective biodiesel, process parameters such as methanol-to-oil ratio, catalyst loading, and reaction temperature will be discussed in this paper. The reaction conditions of various biodiesel production catalysts are summarised in Table 2.1 as shown below (Shuit et al., 2013).

Table 2.1: Comparison of reaction conditions of a number of biodiesel production catalysts (Shuit et al., 2013).

	Reaction conditions						
	Feedstock	**Catalyst used**	**Temperature (℃)**	**Methanol-to-oil molar ratio**	**Catalyst loading (wt%)**	**Time (hour)**	**Yield (%)**
Homogeneous base	Sunflower oil	NaOH	60.0	6:1	1.00	2.00	97.0
Homogeneous acid	Soybean oil	H_2SO_4	65.0	30:1	1.00	50.00	Conversion >99
	Waste cooking oil	H_2SO_4	95.0	20:1	4.00	10.00	Conversion >90
Heterogeneous base	Soybean oil	γ-Al_2O_3	60.0	9:1	2.30	2.00	83.0
	Glyceryl tributyrate	Et_3N-CNT	60.0	12:1	2.00	8.00	77.0
	Soybean oil	Ba/ZnO	65.0	12:1	6.00	1.00	Conversion = 95.0
	Soybean oil	KF/ZnO	65.0	10:1	3.00	9.00	Conversion = 87.0
	Soybean oil	MgO (III)	200.0	11:1	5.00	1.00	>95.0
	Soybean oil	CHT	200.0	11:1	5.00	1.00	>95.0
	Crude coconut oil	KNO_3/KL zeolite	200.0	6:1	3.00	4.20	77.0
	Crude coconut oil	KNO_3/ZrO_2	200.0	6:1	3.00	4.20	66.0

	Crude coconut oil	ZnO	200.0	6:1	3.00	4.20	78.0
Heterogeneous acid	Oleic acid	HMFI (25) zeolites	60.0	15:1	5.60	1.00	85.0
	Oleic acid	s-MWCNTs	135.0	6.4:1	0.20	1.50	Conversion = 96.0
	Soybean oil	VOP	150.0	27:1	6.50	1.00	80.0
	Acidic sunflower oil	Fe-Zn-1	170.0	15:1	3.00	8.00	Conversion = 98.0
	Crude coconut oil	SO_4/SnO_2	200.0	6:1	3.00	4.20	81.0
	Sesame oil	15 WZ-750	200.0	20:1	3.00	5.00	97.0
	Soybean oil	WZ	250.0	40:1[a]	6.70[a]	4.00	Conversion >96.0
	Cottonseed oil	SO_4^{2-}/ZrO_2	230.0	12:1	2.00	8.00	>90.0
	Purified palm oil	SO_4^{2-}/ZrO_2	250.0	24:1	0.50	10 min	Conversion = 90.0
	Palm fatty acid	SO_4^{2-}/ZrO_2	250.0	6:1	0.50	1 min	Conversion = 75.0
	Soybean oil	SZA	300.0	40:1[a]	6.70[a]	4.00	80.0

[a] Self-estimation.

2.6.1 Methanol-to-Oil Ratio

Methanol-to-oil ratio is one of the essential process parameters in synthesizing biodiesel. From the stoichiometric equation, transesterification reaction requires three moles of methanol and one mole of triglyceride. In the meantime, only one mole of methanol and one mole of fatty acid are required for esterification (Marchetti et al., 2007). Since both are reversible reactions, excess methanol is required in order to drive the reaction forward, enhancing the FAME formation (Shuit et al., 2012).

Villa et al. (2010a), investigated the transesterification catalyzed by Et_3N-CNT as catalyst using different molar ratio of methanol to glyceryl tributyrate (6:1, 12:1, 24:1, and 60:1). It was found that the higher the amount of methanol, the more active the system is. For molar ratios of 24:1, and 60:1, complete conversion was achieved in 4 hours and 2 hours, respectively. For molar ratios of 12:1, a conversion of 77 % was achieved after 8 hours. In comparison, for molar ratios of 6:1, deactivation of catalyst was observed.

During transesterification and esterification, protonation occurs at the carboxyl group of the chemisorbed molecule, which will then be attacked by methanol to form FAME. When there is a surplus of methanol, the attack of methanol is enhanced, leading to higher yield of FAME. Nevertheless, when the methanol to oil ratio to too high, the active sites of the catalyst will be flooded by the surplus of methanol instead of oil (Shu et al., 2009). In addition, when the methanol-to-oil ratio increases, the separation difficulty and complexity increases (de Boer and Bahri, 2011).

2.6.2 Reaction Temperature

Villa et al. (2010a), studied the influence of reaction temperature on the catalytic activity using amino-functionalized MWCNTs as catalyst for the transesterification of glyceryl tributyrate with methanol. It was found that when the reaction temperature is high, the conversion and rate of conversion increases. However, more

energy was required to maintain the reaction at high temperatures. Hence, a lower temperature is more preferable. Unfortunately, too low a temperature would result in lower conversion and longer reaction time. The other basic catalysts listed in Table 2.1 shows the similar results (Shuit et al., 2013).

2.6.3 Reaction Time

For the study carried out by Villa et al. (2010a), the reaction time for the transesterification was significantly influenced by the temperature of the reaction and methanol-to-oil ratio used. When reaction temperature and methanol-to-oil ratio increase, there was an increase in catalytic activity and the reaction time was greatly reduced. It was believed that there will be a reduction in reaction time as well when the catalyst loading increasing. The reason for this is because there are more active sites accessible for the reaction to take place.

Shuit et al. (2013), reported that the longer reaction times, the higher the conversion or yield of biodiesel, up until the chemical equilibrium is accomplished, regardless of the types of catalyst and the technologies used. When the methanol to oil ratio and catalyst loading are fixed, the reaction time required to achieve complete conversion is two hours when the temperature is augmented to 90 ℃. When the temperature is reduced to 75 ℃, 6 h is required for 90 % conversion and so on.

CHAPTER 3

METHODOLOGY

3.1 Materials

3.1.1 Raw Materials

PFAD used in this thesis was provided by a local edible oil manufacturing company. Graphite was bought from Shenzhen Nanotechnologies Port Co.

3.1.2 Chemicals

All the chemicals utilized in this project were listed in Table 3.1 with thorough information of purity, name of suppliers and purpose of use.

Table 3.1: Lists of chemical reagents used.

Chemicals	Purity (%)	Supplier	Purpose of use
Acetic anhydride ($(CH_3CO)_2O$)	99	Acros Organics, Malaysia	Sulfonation of graphite and as drying agent during preparation of polymer
n-Hexane	99	Fischer Scientific, Malaysia	Solvent for gas chromatography (GC) analysis

Methanol (CH_3OH)	99	Fischer Scientific, Malaysia	Esterification reaction and preparation of polymer
Methyl heptadecanoate	99	Sigma-Aldrich, Malaysia	Internal standard for GC analysis
Sulfuric acid (H_2SO_4)	N/A	Fischer Scientific, Malaysia	Sulfonation of graphite
Nitric acid (HNO_3)	N/A	JT Baker, Malaysia	Purification of graphite
Methyl linoleate	99	Fluka Chemie, Germany	Internal standard for GC analysis

3.2 Preparation of Catalyst

The purification and sulfonation of graphite in this study were performed parallel to the method described by Peng et al. (2005) and Shuit and Tan (2015) as graphite has nearly similar properties as carbon nanotubes. Due to limited references on the using of sulfonated graphite as the acid solid catalyst, the operating conditions for MWCNTs will be used as the reference in this study.

3.2.1 Purification of Pristine Graphite

Initially, a mixture of graphite (1 g) and HNO_3 (100 ml) was ultrasonicated for 1 h and followed by refluxing at 80 ℃ for 8 h. The treated graphite was then filtered and washed by distilled water (DW) until the pH of the filtrate matched with the pH of DW. The graphite was then dried at about 120 ℃ for 12 h to obtain graphite-COOH, before being sulfonated.

3.2.2 Sulfonation of by Polymerisation of Sulfuric Acid and Acetic Anhydride

The sulfonation procedures and the amount of chemicals used are based on those reported by Sun et al. (2009) and Ramulifho et al. (2012). In this process, 0.2 g of graphite-COOH was added into a mixture containing $(CH_3CO)_2O$ and 20 ml of concentrated H_2SO_4. The mixture was then stirred and heated to 70 ℃ for 2 h. Next, the mixture was cooled down to room temperature while stirring continuously. The resultant products was then filtered was then and washed by using DW until the pH of the filtrate matched with the pH of DW. It was then dried at 120 ℃ for 12 h. The sulfonated graphite was denoted as s-graphite.

3.3 Esterification

The esterification of PFAD into FAME (biodiesel) was conducted in a three-round-neck glass reactor furnished with a thermocouple and a magnetic stirrer. Before 10 g of PFAD was added, a pre-determined amount of s-graphite was stirred in methanol for 10 min to avoid the adsorption of PFAD to the active sites that would lead to catalyst deactivation (Villa et al., 2010b). In this study, the molar ratios of methanol to PFAD were 5, 17.5 and 30. The reaction temperature were set at 80, 125 and 170 ℃. In addition, the catalyst loadings used were 1.0, 2.0 and 3.0 wt% (based on the mass of PFAD). The reactants were stirred at 300 rpm to maintain a constant temperature and uniform suspension. For each set of the parameters (methanol-to-PFAD ratio, reaction temperature and catalyst loading), the reaction time for the esterification was fixed to be 3 h. Reaction time was counted when the desired reaction temperature was achieved and stable. Finally, the reaction mixture was cooled to room temperature and filtered to separate s-graphite from the reaction mixture. A rotary evaporator was used to remove the excess methanol.

3.4 FAME Analysis

A gas chromatograph fitted with a flame ionization detector (FID) and a capillary column were utilised to analyse the composition and the yield of FAME or biodiesel. n-Hexane and helium were used as the solvent and carrier gas, respectively. The oven temperature was first set to be 110 ℃ and steadily increased at a rate of 10 ℃/min to 210 ℃. The temperature of the detector and injector were set at 210 and 240 ℃, respectively. The internal standard used was methyl heptadecanoate (Shuit et al., 2010). The following equation was used to calculate the yield of FAME in the samples:

$$\text{Yield}\ (\%) = \frac{(\sum \text{Concentration of each FAME}, \frac{\text{g}}{\text{cm}^3}) \times (\text{Volume}, \text{cm}^3)}{10\ \text{g of PFAD}} \times 100\%$$

3.5 Characterization Methods

3.5.1 X-Ray Diffraction (XRD) Analysis

Wide angle XRD measurements of the s-graphite were carried out by a Shimadzu XRD-6000 at room temperature with CuKα radiation operated at 40 kV and 30 mA. The diffraction angle was set from 20 to 90 ℃ with a sweep rate of 0.04 °/s. The average interspacing distance between layers (d-space) was reflected by the broad peak centred on each X-ray pattern. The average d-spacing for the s-graphite was calculated based on Bragg's law as shown in the following equation:

$$n\lambda = 2dsin\theta$$

where

n = number of order

λ = wavelength of X-ray

d = lattice plane distance

θ = diffraction angle

Besides, Debye-Scherrer equation is used to determine the size of the crystallites. The equation is as shown below.

$$\tau = \frac{0.89\lambda}{FWHM \times cos\ \theta}$$

where

τ = crystallite size

λ = wavelength of X-ray

FWHM = full length at half maximum (line width)

θ = diffraction angle

3.5.2 Scanning Electron Microscopy (SEM) Spectroscopy

The surface and structure morphology of the s-graphite after the thermal treatment were observed by using a Hitachi S-3400N.

3.5.3 Fourier Transform-Infrared (FT-IR) Spectroscopy

The presence of the sulfonic (SO_3H) groups was validated by the FT-IR analysis using a Shimadzu IRPrestige-21 over a frequency range of 4000-500 cm^{-1}. A blend of s-graphite sample and potassium bromide was pelleted into a tiny pellet, and the IR spectrum was collected after 32 scans. On the other hand, the structure of the s-graphite was confirmed by using the attenuated total reflectance (ATR) mode.

CHAPTER 4

RESULTS AND DISCUSSION

4.1 Characterization of Catalyst

4.1.1 XRD Analysis

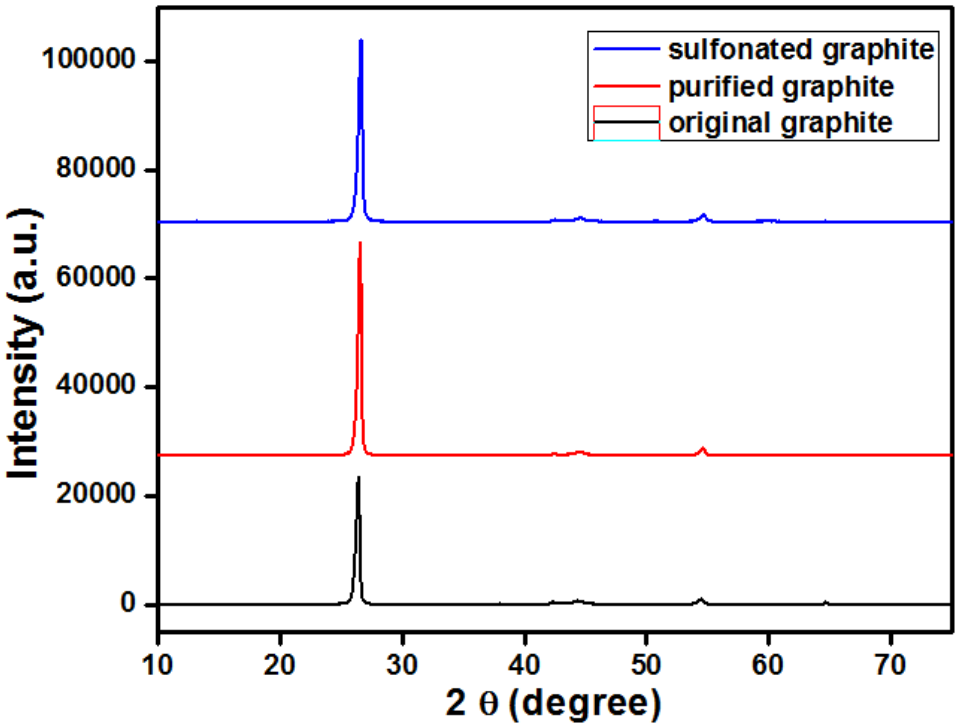

Figure 4.1: XRD patterns for graphite of different preparation conditions.

Note: The combined XRD patterns were generated using software called OriginPro.

The XRD patterns in Figure 4.1 show the characteristics reflection of the crystalline structures of graphite catalyst under three different preparation conditions. The three types of catalysts used consisted of original graphite, purified graphite by using nitric acid, and sulfonated graphite by using a mixture of H_2SO_4 and $(CH_3CO)_2O$. All three of the well-crystallized graphite catalysts give two main characteristic peaks. Liaw (2013) proved that the peak around 20^o were assigned to the graphitic [0 0 2] planes.

The development of the crystalline structure formation of the surface morphology is influenced by the preparation conditions of catalysts. The original graphite catalyst was expected to give larger crystallite sizes than both the purified and sulfonated graphite catalysts. Meanwhile, the sulfonated graphite catalyst was estimated to give smallest crystallite sizes due to its harsher preparation conditions compared to the other two catalysts. Smaller crystallite sizes give better catalytic activities because they are sharper for the sulfonic ($-SO_3H$) groups to graft on them. Moreover, larger crystallite sizes tend to take up more space than smaller crystallite sizes and consequently, lowers down the number of actives sites available and decreasing the biodiesel production.

From XRD data, the crystallite size of catalyst can be determined. The detailed data and graphs generated by using XRD for all three types of catalysts will be enclosed in Appendix A. Table 4.1 below shows the basic data extracted from Appendix A for the purpose of calculation and discussion.

Table 4.1: Basic data extracted from XRD

Catalyst	Peak	2θ (deg)	FWHM (deg)	Integrated intensity (counts)
Original	1	26.3464	0.41830	324763
	2	54.3802	0.52900	17499
Purified	1	26.4928	0.36890	514488
	2	54.5125	0.49170	26844
Sulfonated	1	26.5540	0.42540	480543
	2	54.5716	0.54040	26603

From Table 4.1, it clearly shows that the integrated intensity for both purified and sulfonated graphite catalysts are much higher than the original graphite catalyst. This confirms the need and importance of catalyst preparation methods because higher integrated intensity means higher amount of crystalline structures present. Therefore, this will in turn increase the catalytic activity and biodiesel yield. Unfortunately, the integrated intensity for sulfonated graphite was lesser than that of purified graphite. The most probable reason for this phenomenon was due to the sintering effect during refluxing or prolonged drying in an oven. Nevertheless, its integrated intensity was much higher than the original graphite and not too low than the purified graphite.

The size of crystallites was determined by using Debye-Scherrer equation. Peak 1 of original graphite catalyst was taken as the sample calculation. The wavelength, λ of X-rays is fixed at 1.54 Å.

$$\tau = \frac{0.89\lambda}{FWHM \times cos\,\theta} = \frac{1.3706}{FWHM \times \cos\theta} = \frac{1.3706}{\left(0.4183 \times \frac{\pi}{180}\right) \times \left(cos\ \frac{26.3464}{2}\right)}$$

$$= 192.81\ \text{Å}$$

The Table 4.2 shows the computed crystallite sizes for all peaks of the three catalysts. It shows a trend where crystallite sizes of the catalysts decrease with harsher preparation conditions. This shows that sulfonated graphite catalyst was better than the other two catalysts since it offered greater catalytic activity.

Table 4.2: Computed crystallite sizes for graphite catalysts

Catalyst	Crystallite size, τ (Å)	
	Peak 1	Peak 2
Original	192.81	166.89
Purified	190.69	164.66
Sulfonated	189.67	163.51

4.1.2 SEM Spectroscopy

(a) Original graphite catalyst

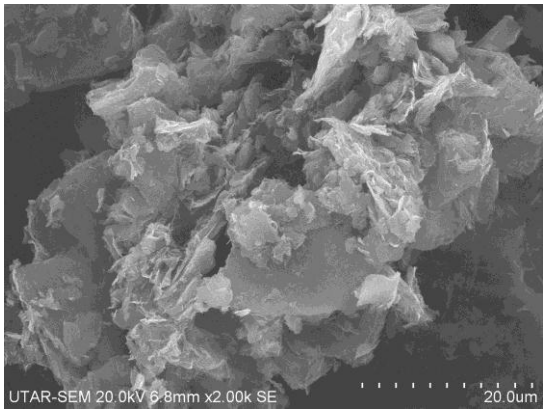

(b) Purified graphite catalyst

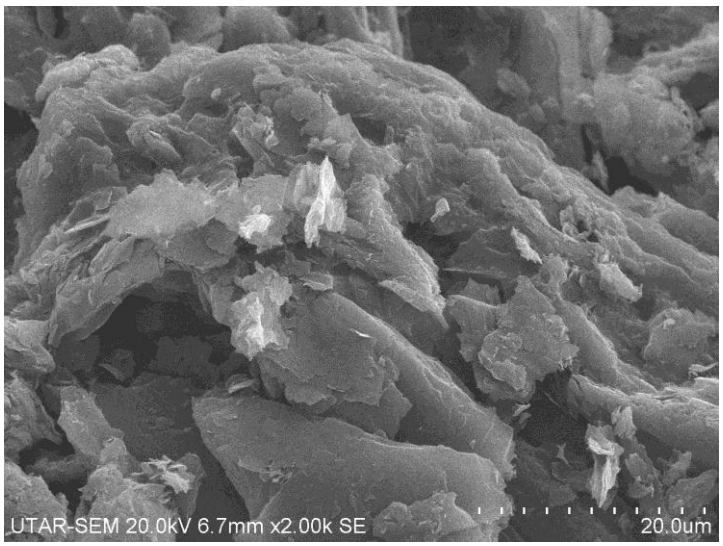

(c) Sulfonated graphite catalyst

Figure 4.2: SEM images with magnification of ×2.0k for (a) original graphite, (b) purified graphite and (c) sulfonated graphite catalyst.

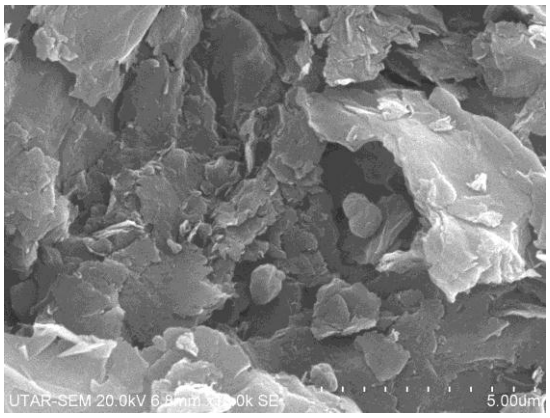

(a) Pristine graphite catalyst

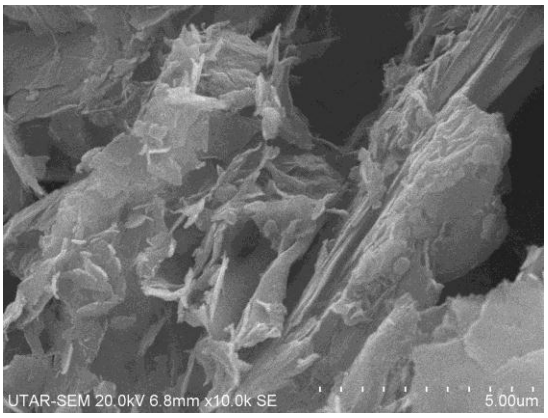

(b) Purified graphite catalyst

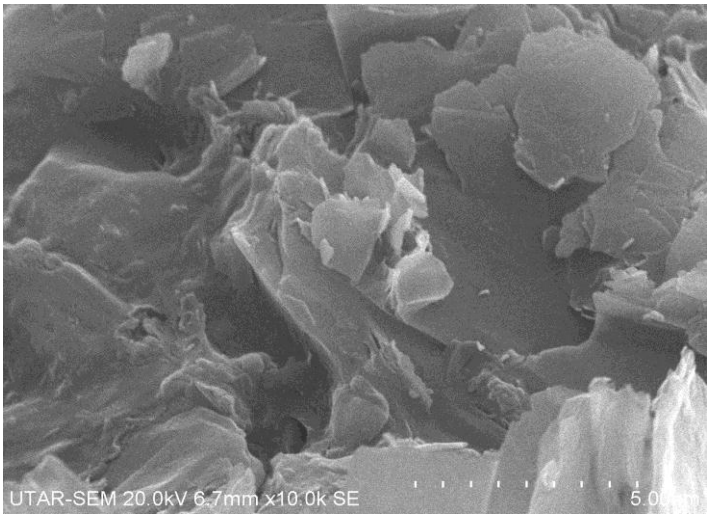

(c) Sulfonated graphite catalyst

Figure 4.3: SEM images with magnification of ×10.0k for (a) original graphite, (b) purified graphite and (c) sulfonated graphite catalyst.

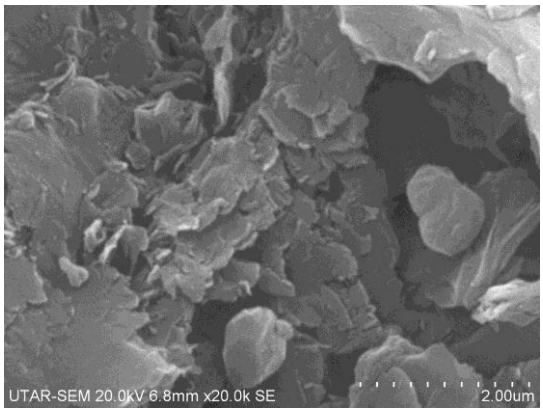

(a) Pristine graphite catalyst

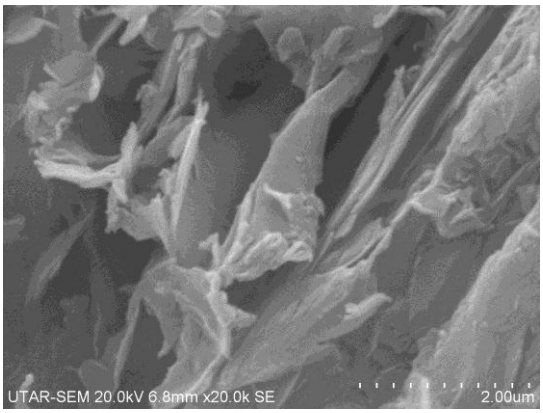

(b) Purified graphite catalyst

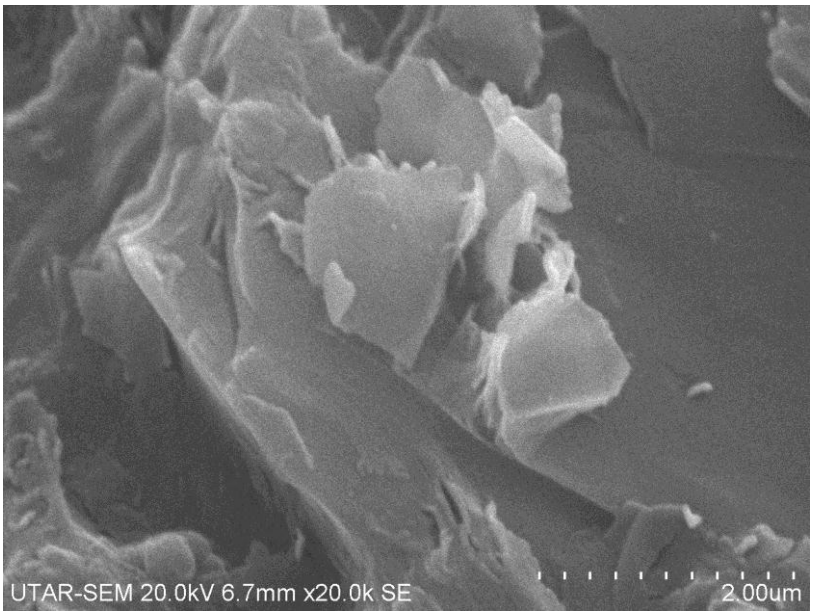

(c) Sulfonated graphite catalyst

Figure 4.4: SEM images with magnification of ×20.0k for (a) original graphite, (b) purified graphite and (c) sulfonated graphite catalyst.

Figure 4.2, Figure 4.3 and Figure 4.4 show the SEM images for pristine graphite, purified graphite and sulfonated graphite catalyst with magnifications of ×2.00k, ×10.0k and ×20.0k, respectively. The results of SEM spectroscopy show the surface morphologies of graphite catalyst based on different preparation conditions. The basic structure of graphite catalyst is its planar sheets of different thickness.

From the SEM images of different magnifications, it can be observed that the purified graphite catalyst has more cracks and defects than the pristine graphite catalyst. Meanwhile, the sulfonated graphite catalyst has the highest amount of cracks and defects than the other two catalysts. This is due to the harsher preparation conditions of the graphite catalyst since it involved a two-step process consisting of both purification and sulfonation. The cracks and defects present will become the active sites of the catalyst for the sulfonic groups to anchor on and form chemical bonds. Therefore, sulfonated graphite catalyst is a better catalyst than the others because it has higher number of sulfonic groups to catalyze chemical reactions and increase the biodiesel yield.

4.1.3 FT-IR Spectroscopy

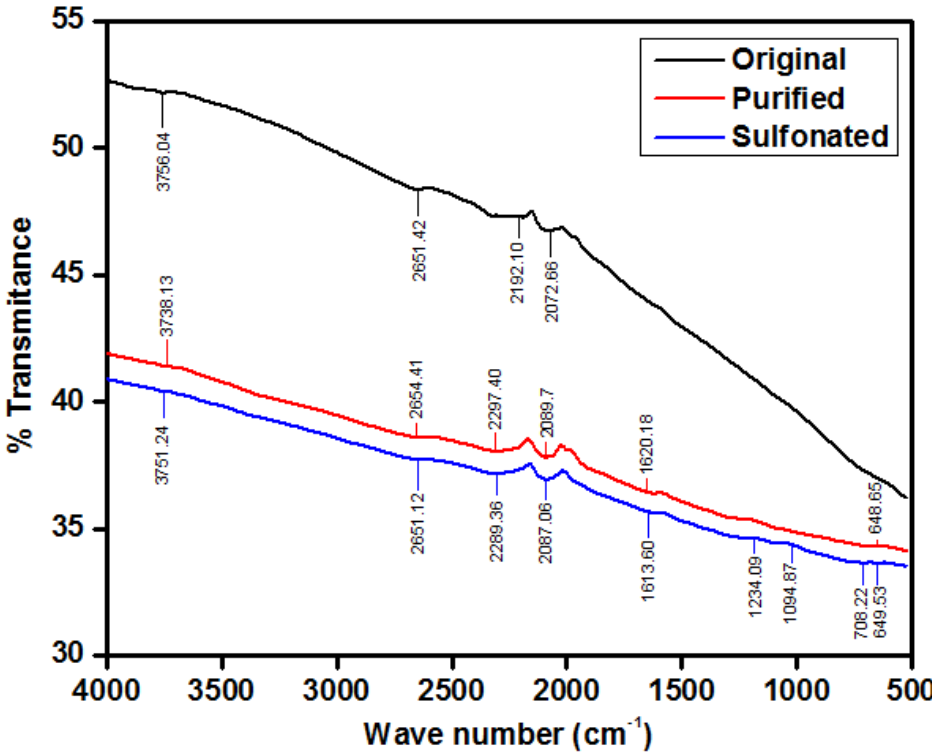

Figure 4.5: FTIR spectra of original, purified and sulfonated graphite.

Note: The FTIR spectra were generated by using software called OriginPro and the enlarged figure will be provided in Appendix B.

Figure 4.5 shows the IR spectra of original, purified and sulfonated graphite catalyst in the range of 500-4000 cm^{-1}. The spectra show significant differences between all three types of graphite catalyst. The peak at around 3750 cm^{-1} indicates the presence of –OH groups (Lam et al., 2010). The formation of –OH groups on the catalyst is very advantageous because it enhances the catalytic activities of the solid acid catalysts (Shuit and Tan, 2014). The peak at about 1600 cm^{-1} and was assigned to the aromatic-like C=C stretching mode in polyaromatic sketch (Liaw, 2013). The peaks at 1234.09, 1094.87 and 649.53 cm^{-1} only appear in the spectra of sulfonated graphite catalyst. The presence of sulfonate groups was indicated by the peak at 1234.09 cm^{-1}. Furthermore, the absorption peak at 1094.87 cm^{-1} was attributed to the asymmetric and symmetric O=S=O stretching vibrations, and the peak at 649.53 cm^{-1} indicated the presence of S-O groups on the surface of the catalyst (Shuit and Tan, 2014). In a conclusion, the FT-IR spectra showed the capability of introducing SO_3H groups on the surfaces of graphite catalyst through the chosen sulfonation method.

4.2 Optimization of Biodiesel (Numerical Calculation)

4.2.1 Methanol-to-PFAD Ratio

Table 4.3 shows the influence of different methanol-to-PFAD ratio on the FAME yield at the fixed reaction temperature of 170 ℃ and a fixed catalyst loading of 3 wt%. The range methanol-to-PFAD ratio used in this study was between from 5.0 to 30.0.

Table 4.3: Effect of the methanol-to-PFAD ratio on the FAME yield

Ratio	Yield (%)
5.0	23.24712
17.5	53.14844
30.0	95.0616

A graph of yield versus methanol-to-PFAD ratio was plotted and depicted by Figure 4.6. From the trend result, it suggested that the optimal methanol-to-PFAD ratio was at 30.0.

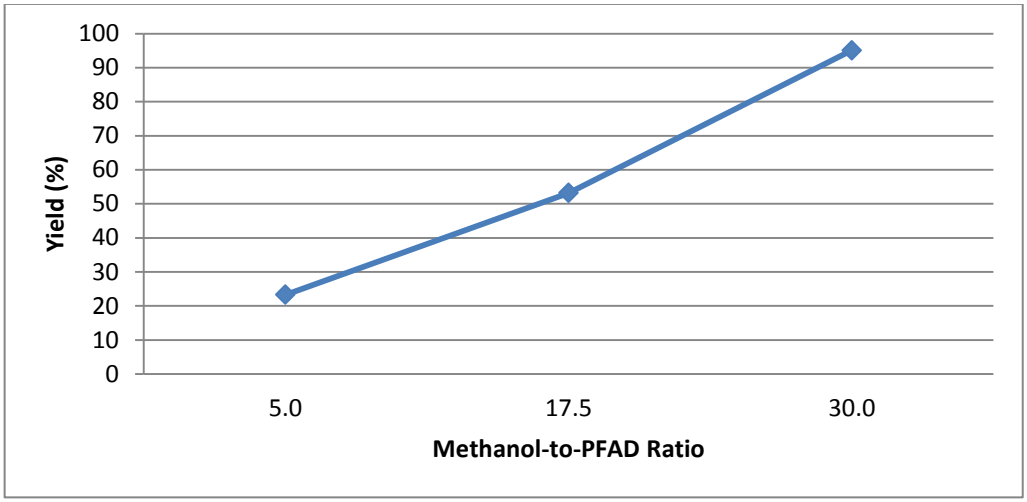

Figure 4.6: The effect of methanol-to-PFAD ratio on the biodiesel yield.

The reason for such a trend was because when the methanol-to-PFAD ratio increases, there are more methanol molecules to react with PFAD molecules attached on the catalyst surface. Hence, more esterification reactions will take place, leading to higher yield of biodiesel. However, the methanol-to-PFAD ratio cannot be too high as the number of PFAD molecules present on catalyst is limited. Otherwise, it will lead to the saturation of the active sites of graphite catalyst by methanol molecules, giving a lower biodiesel yield. That being said, further study should be carried out by increasing the number of set values in order to determine the optimum value of methanol-to-PFAD ratio which gives the highest biodiesel yield.

4.2.2 Reaction Temperature

Table 4.4 shows the effect of different reaction temperature on the FAME yield at the fixed methanol-to-PFAD ratio of 17.5 and a fixed catalyst loading of 2 wt%. The range of reaction temperature used in this study was between 80 and 170 ℃.

Table 4.4: Effect of the reaction temperature on the FAME yield.

Reaction Temperature (℃)	Yield (%)
80	30.16244
125	31.54816
170	32.08473

A graph of yield versus reaction temperature was plotted and depicted by Figure 4.7. From the trend result, it suggested that the optimal reaction temperature was 170 ℃.

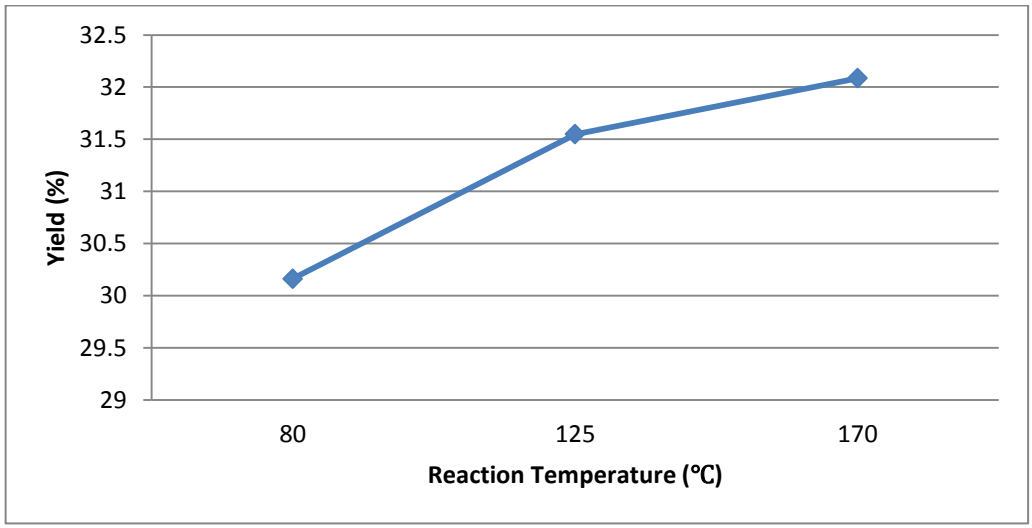

Figure 4.7: The effect of reaction temperature on the biodiesel yield.

The reason for such a trend was because when reaction temperature increases, the reacting molecules gain kinetic energy and react faster. The number and frequency of effective collisions between methanol and PFAD will increase significantly, giving rise to higher yield of biodiesel. However, the reaction temperature cannot be too high because it will need higher heating requirement. Hence, higher production cost is required and it will increase the risk of fire and explosion from a safety point of view. That being said, further study should be carried out by increasing the number of set values in order to determine the optimum value of reaction temperature which gives the highest biodiesel yield.

4.2.3 Catalyst Loading

Table 4.5 shows the effect of different catalyst loading on the FAME yield at the fixed methanol-to-PFAD ratio of 17.5 and a fixed reaction temperature of 125 ℃. The catalyst loading was increased from 1 to 3 wt%.

Table 4.5: Effect of the catalyst loading on the FAME yield.

Catalyst Loading (wt%)	Yield (%)
1.0	33.97525
2.0	35.14844
3.0	37.79040

A graph of yield versus catalyst loading was plotted and depicted by Figure 4.8. From the trend result, it suggested that the optimal catalyst loading was at 3.0 wt%.

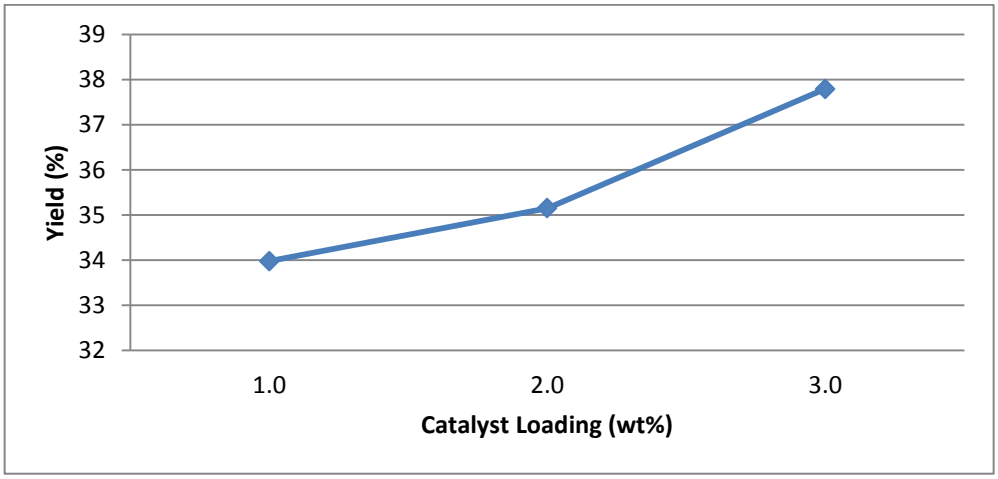

Figure 4.8: The effect of catalyst loading on the biodiesel yield.

The reason for such a trend was because when the catalyst loading increases, there are more catalysts present. More catalysts present mean more number of active sites present, carrying the PFAD molecules. Hence, methanol

molecules can react easily and actively with the PFAD molecules, leading to higher activity and biodiesel yield. However, the catalyst loading cannot be too high because the number of methanol molecules present is limited for them to react with PFAD molecules attached on the catalyst. When the catalyst loading is too high, the reaction is said to be saturated by the catalyst, leading to lower yield of biodiesel. That being said, further study should be carried out by increasing the number of set values in order to determine the optimum value of reaction temperature which gives the highest biodiesel yield.

4.3 Optimization of Biodiesel (Software Calculation)

Apart from the conventional manual calculation, a reliable analysis can also be done by using software called DesignExpert8. This software design was based on the response surface and central composite designs with three changing parameters namely: methanol-to-PFAD ratio, reaction temperature and catalyst loading. Meanwhile, the biodiesel yield was set to be the response. Table 4.6 shows the results for the all of the experiment runs. At the first glance, it is obvious that run 20 was the outliers of these data. Thus, this may influence the subsequent analysis.

Table 4.6: Biodiesel yield for different parameters.

Run	Temperature (℃)	Catalyst Loading (wt%)	Methanol-to-PFAD Ratio	Yield (%)
1	80.0	1.00	5.00	52.1407
2	80.0	1.00	30.0	14.46195
3	80.0	2.00	17.5	50.16244
4	80.0	3.00	5.00	9.067411
5	80.0	3.00	30.0	22.23472
6	125.0	1.00	17.5	33.97525
7	125.0	2.00	5.00	45.03471
8	125.0	2.00	17.5	27.60396

9	125.0	2.00	17.5	31.54816
10	125.0	2.00	17.5	35.14844
11	125.0	2.00	17.5	28.35939
12	125.0	2.00	17.5	34.8295
13	125.0	2.00	17.5	30.1926
14	125.0	2.00	30.0	36.06577
15	125.0	3.00	17.5	20.7904
16	170.0	1.00	5.00	12.57012
17	170.0	1.00	30.0	19.61645
18	170.0	2.00	17.5	32.08473
19	170.0	3.00	5.00	23.24712
20	170.0	3.00	30.0	95.0616

4.3.1 Analysis of Test Models

In order to select the best model for this design, the sequential sum of squares test and the lack of fit test were utilized for analysis. The sequential sum of squares test shows how terms of increasing complexity contribute to the total model. To select the best model based on the sequential sum of squares, the probability should be less than 0.05 (<0.05) while the probability for the lack of fit test should be more than 0.05 (>0.05). As shown in Figure 4.9, the p-value for the suggested 2FI (two-factor interaction) vs. Linear is 0.0001 (<0.05), and it gives the best fit. 2FI vs Linear means that the two-factor interaction is also considered in addition to the mean, block and linear terms. Note that the Cubic vs. Quadratic model is not chosen as the terms are aliased.

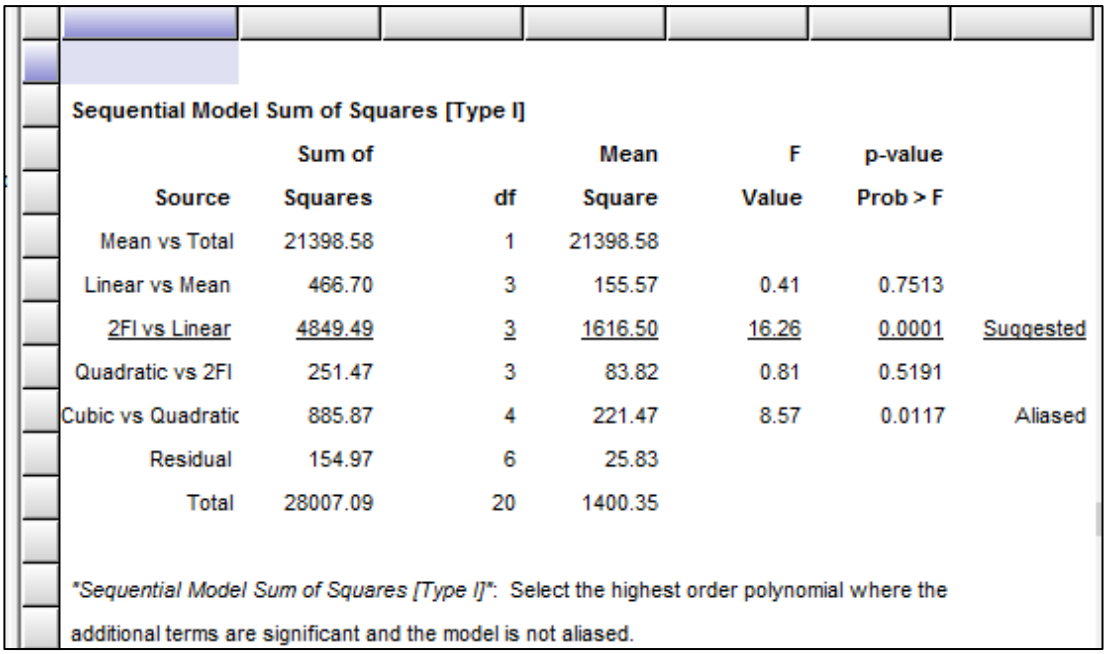

Sequential Model Sum of Squares [Type I]

Source	Sum of Squares	df	Mean Square	F Value	p-value Prob > F	
Mean vs Total	21398.58	1	21398.58			
Linear vs Mean	466.70	3	155.57	0.41	0.7513	
2FI vs Linear	4849.49	3	1616.50	16.26	0.0001	Suggested
Quadratic vs 2FI	251.47	3	83.82	0.81	0.5191	
Cubic vs Quadratic	885.87	4	221.47	8.57	0.0117	Aliased
Residual	154.97	6	25.83			
Total	28007.09	20	1400.35			

*"Sequential Model Sum of Squares [Type I]": Select the highest order polynomial where the additional terms are significant and the model is not aliased.

Figure 4.9: Results of sequential model sum of squares test.

Note: The figure was extracted from the software

As for the lack of fit test shown in Figure 4.10, the greatest p-value (excluding the cubic model) is 0.0041 for the suggested 2FI model. Even though it is not >0.05, it is still the best model to fit. However, caution should be taken if this model is used for response predictor. Note that the cubic model is not chosen as the terms are aliased.

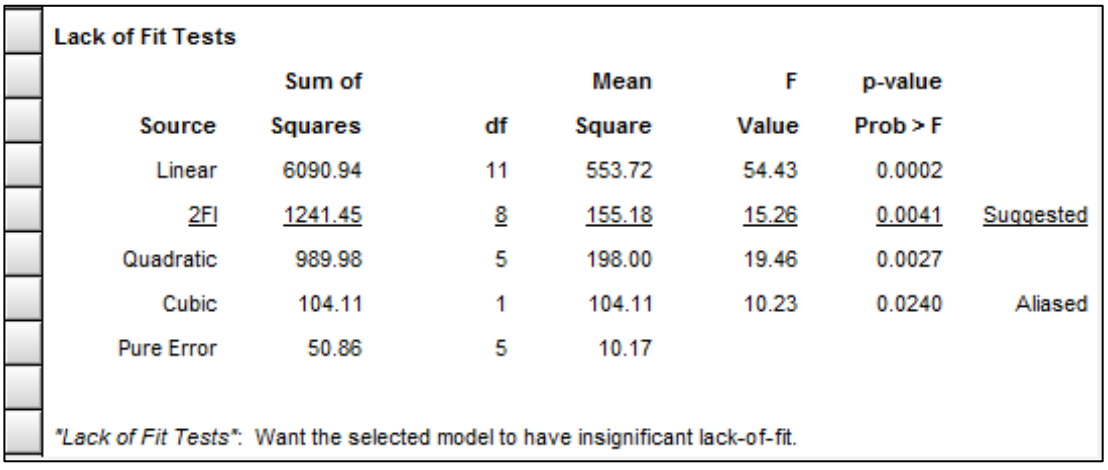

Lack of Fit Tests

Source	Sum of Squares	df	Mean Square	F Value	p-value Prob > F	
Linear	6090.94	11	553.72	54.43	0.0002	
2FI	1241.45	8	155.18	15.26	0.0041	Suggested
Quadratic	989.98	5	198.00	19.46	0.0027	
Cubic	104.11	1	104.11	10.23	0.0240	Aliased
Pure Error	50.86	5	10.17			

*"Lack of Fit Tests": Want the selected model to have insignificant lack-of-fit.

Figure 4.10: Results of lack of fit test.

Note: The figure was extracted from the software

4.3.2 ANOVA Analysis

Figure 4.11 shows the ANOVA results of the design. Important and significant figures to look out for are the p-values of both the model and the lack of fit. The p-value of the model should be less than 0.05 (<0.05). Values outside more than 0.05 mean that the model terms are insignificant. In this case, the significant terms are AB, AC and BC, indicating that the terms interact with each other for this design. The ideal p-value of the lack of fit should be more than 0.05 (>0.05). From the results shown, the p-value is 0.0014 (<0.05). This suggests that the data may not fit in the model. This may be caused by some outliers in the data.

Response 1 Yield

ANOVA for Response Surface 2FI Model

Analysis of variance table [Partial sum of squares - Type III]

Source	Sum of Squares	df	Mean Square	F Value	p-value Prob > F	
Model	5316.19	6	886.03	8.91	0.0005	significant
A-Temperatu	*119.11*	*1*	*119.11*	*1.20*	*0.2935*	
B-Loading	*141.65*	*1*	*141.65*	*1.42*	*0.2539*	
C-Ratio	*205.94*	*1*	*205.94*	*2.07*	*0.1737*	
AB	*1842.93*	*1*	*1842.93*	*18.54*	*0.0009*	
AC	*1335.73*	*1*	*1335.73*	*13.44*	*0.0029*	
BC	*1670.83*	*1*	*1670.83*	*16.81*	*0.0013*	
Residual	1292.32	13	99.41			
Lack of Fit	*1241.45*	*8*	*155.18*	*15.26*	*0.0041*	*significant*
Pure Error	*50.86*	*5*	*10.17*			
Cor Total	6608.51	19				

Figure 4.11: ANOVA table.

Note: The figure was extracted from the software

4.3.3 DFFITS Analysis

The DFFITS analysis can show how influential a point is in the model. From Figure 4.12, two points are out of the range (-2.00 – 2.00). These points correspond to the outliers of the data (run 4 and run 6). The whole model may be heavily influenced by these two points which may not give an accurate prediction.

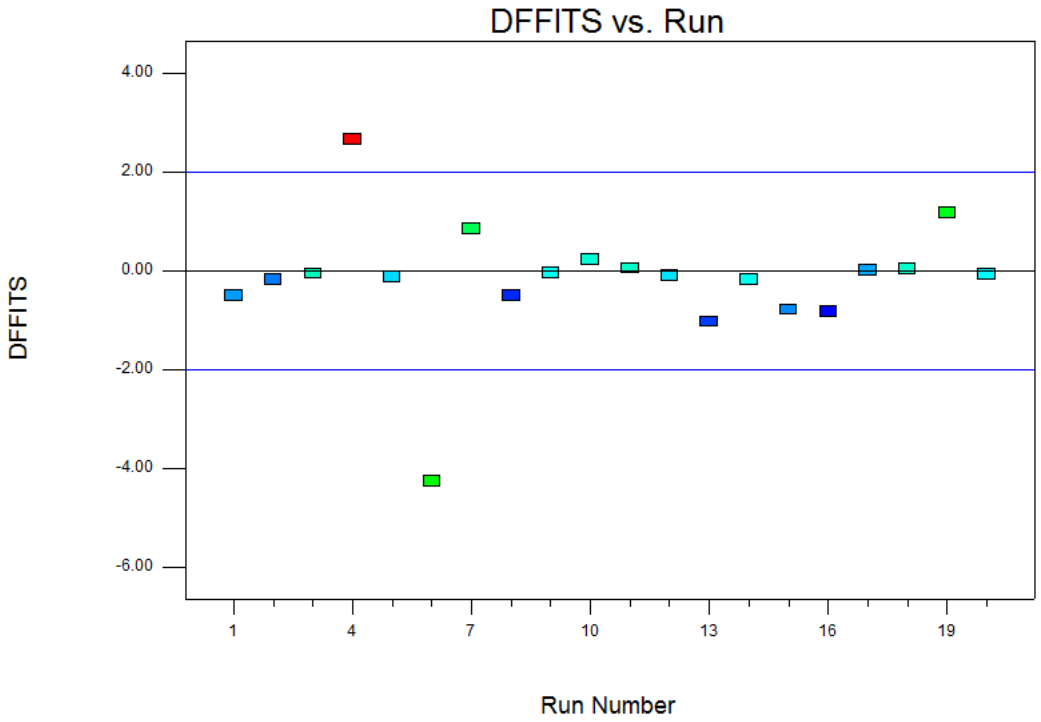

Figure 4.12: Graph of DFFITS vs. Run

Note: The figure was extracted from the software

4.3.4 Contour Plot and 3D Surface Model

Figure 4.13 shows the contour plot while Figure 4.14 shows the 3D surface of the model with reaction temperature and catalyst loading as the x-axes. The reference point was methanol-to-PFAD ratio and was set at 17.5. From the contour plot and 3D surface model, it was suggested that the yield of biodiesel is higher either from a combination of low temperature and low catalyst loading or high temperature and high catalyst loading are used. Since the two outliers involve Run 4 (80 ℃, 3 wt%, 5)

and Run 6 (125 ℃, 1 wt%, 17.5), the combination of low temperature and low catalyst loading might not be the accurate depiction for high biodiesel yield. Therefore, high temperature and high catalyst loading is more preferable since it offers a more accurate analysis. This is tally with the manual calculation where the optimal reaction temperature is 170 ℃ and the catalyst loading is 3 wt%.

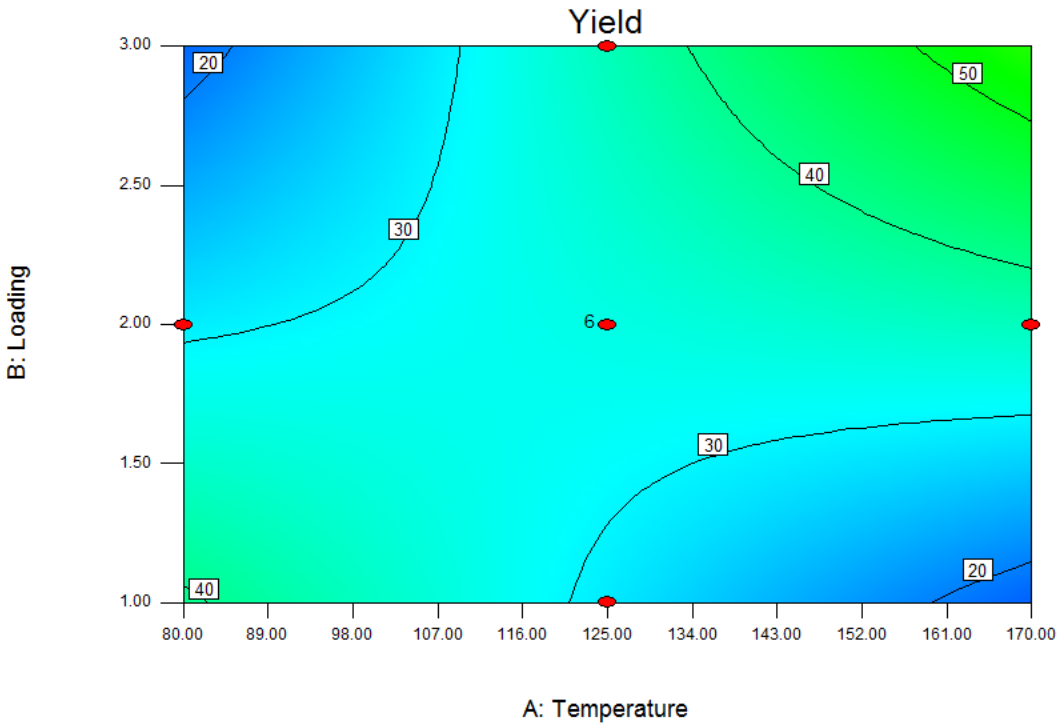

Figure 4.13: Contour plot.

Note: The figure was extracted from the software

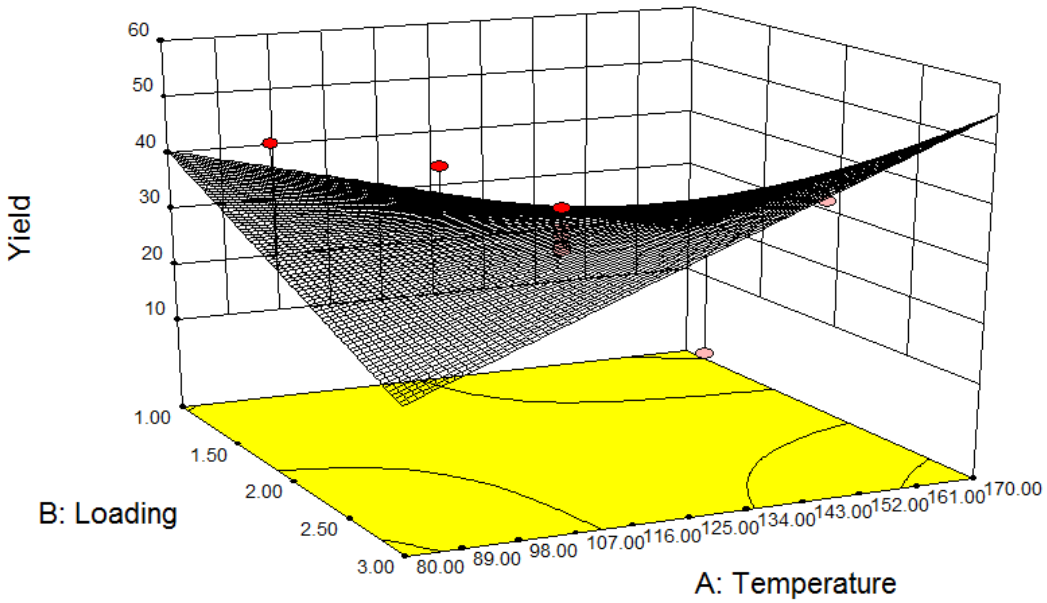

Figure 4.14: 3D surface model.

Note: The figure was extracted from the software

CHAPTER 5

CONCLUSION AND RECOMMENDATIONS

5.1 Conclusion and Recommendations

In this thesis, the esterification process of PFAD and methanol to form biodiesel was successfully investigated using graphite as catalyst. Catalyst characterization methods such as XRD, SEM and FTIR were completed on the graphite catalysts based on different preparation conditions. The three types of catalyst investigated were original, purified and sulfonated graphite catalysts. Besides that, GC was carried to determine the yield of biodiesel for different process parameters such as methanol-to-PFAD ratio, reaction temperature and catalyst loading. Three sets of data were examined for each of the process parameters.

From the XRD Analysis, all three of the well-crystallized graphite catalysts give two main characteristic peaks. The integrated intensity for both purified and sulfonated graphite catalysts are much higher than the original graphite catalyst. This confirms the need and importance of catalyst preparation methods because higher integrated intensity means higher number of active sites present. The computed crystallite sizes for all peaks of the three catalysts shows a trend where crystallite sizes of the catalysts decrease with harsher preparation conditions. This shows that sulfonated graphite catalyst was better than the other two catalysts since it offered greater catalytic activity and biodiesel yield.

For SEM spectroscopy, it can be observed that the purified graphite catalyst has more cracks and defects than the pristine graphite catalyst. Meanwhile, the

sulfonated graphite catalyst has the highest amount of cracks and defects than the other two catalysts. Therefore, sulfonated graphite catalyst is a better catalyst than the others because it has higher number of sulfonic groups to catalyze chemical reactions and increase the biodiesel yield.

For FT-IR spectroscopy, the presence of sulfonate groups, O=S=O stretching vibrations and S-O groups was only shown in the sulfonated graphite catalyst but not the other two. It showed the capability of introducing SO_3H groups on the surfaces of graphite catalyst through the chosen sulfonation method.

For GC analysis, process parameters such as methanol-to-PFAD ratio, reaction temperature and catalyst loading were selected to investigate their effect on the biodiesel yield and to predict their optimal values. The optimal methanol-to-PFAD ratio, reaction temperature and catalyst loading were 30.0, 170 ℃ and 3 wt%, respectively. These results were tally with the one suggested by using software DesignExpert8 where it was more preferable to have high temperature and high catalyst loading since it offered a more accurate analysis.

5.2 Recommendations

Based on the analysis done in this study, functionalized graphite is very assuring and believed to have the potential to be the ensuring catalyst for use in the production of biodiesel. The limitations of the conventional heterogeneous catalysts such as low stability, mass transfer problem, high cost of catalyst and limited reusability can be improved by using graphite as catalyst support.

Moreover, the number of set values is recommended to be increased for each of the process parameters. This is to confirm a more accurate and reliable results.

REFERENCES

Abbaszaadeh, A., Ghobadian, B., Omidkhah, M.R. & Najafi, G., 2012. Current biodiesel production technologies: A comparative review. *Energy Conversion and Management,* [online] Available at: http://www.sciencedirect.com/science/article/pii/S0196890412001185 [Accessed 20 July 2015].

Alonso, D.M., Mariscal, R., Moreno-Tost, R., Poves, M.D.Z. & Granados, M.L., 2007. Potassium leaching during triglyceride transesterification using K/γ-Al2O3 catalysts. *Catalysis Communications,* [online] Available at: http://www.sciencedirect.com/science/article/pii/S1566736707001410 [Accessed 1 August 2015].

Altic, L.E.P., 2010. *Characterization of the esterification reaction in high free fatty acid oils.* 1482917 M.S.M.E. University of South Florida. Available at: http://search.proquest.com/docview/815248440?accountid=50207 [Accessed 21 July 2015].

Atabani, A.E., Silitonga, A.S., Badruddin, I.A., Mahlia, T.M.I., Masjuki, H.H. & Mekhilef, S., 2012. A comprehensive review on biodiesel as an alternative energy resource and its characteristics. *Renewable and Sustainable Energy Reviews,* [online] Available at: http://www.sciencedirect.com/science/article/pii/S1364032112000044 [Accessed 16 July 2015].

Atadashi, I.M., Aroua, M.K., Abdul Aziz, A.R. & Sulaiman, N.M.N., 2012. Production of biodiesel using high free fatty acid feedstocks. *Renewable and Sustainable Energy Reviews,* [online] Available at: http://www.sciencedirect.com/science/article/pii/S1364032112001578 [Accessed 20 July 2015].

Balasubramanian, K. & Burghard, M., 2005. Chemically Functionalized Carbon Nanotubes. *Small,* [online] Available at: http://dx.doi.org/10.1002/smll.200400118 [Accessed 1 August 2015].

Borges, M.E. & Díaz, L., 2012. Recent developments on heterogeneous catalysts for biodiesel production by oil esterification and transesterification reactions: A review. *Renewable and Sustainable Energy Reviews,* [online] Available at: http://www.sciencedirect.com/science/article/pii/S1364032112000834 [Accessed 31 July 2015].

Chekin, F., Bagheri, S. & Abd Hamid, S.B., 2013. Synthesis of Pt doped TiO2 nanoparticles: Characterization and application for electrocatalytic oxidation of l-methionine. *Sensors and Actuators B: Chemical*, [online] Available at: http://www.sciencedirect.com/science/article/pii/S0925400512013111 [Accessed 31 July 2015].

Chongkhong, S., Tongurai, C., Chetpattananondh, P. & Bunyakan, C., 2007. Biodiesel production by esterification of palm fatty acid distillate. *Biomass and Bioenergy*, [online] Available at: http://www.sciencedirect.com/science/article/pii/S0961953407000554 [Accessed 22 July 2015].

Chuah, G.K., Jaenicke, S. & Xu, T.H., 2000. The effect of digestion on the surface area and porosity of alumina. *Microporous and Mesoporous Materials*, [online] Available at: http://www.sciencedirect.com/science/article/pii/S1387181199002772 [Accessed 30 July 2015].

d'Halluin, M., Mabit, T., Fairley, N., Fernandez, V., Gawande, M.B., Le Grognec, E. & Felpin, F.-X., 2015. Graphite-supported ultra-small copper nanoparticles – Preparation, characterization and catalysis applications. *Carbon*, [online] Available at: http://www.sciencedirect.com/science/article/pii/S0008622315005321 [Accessed 1 August 2015].

de Boer, K. & Bahri, P.A., 2011. Supercritical methanol for fatty acid methyl ester production: A review. *Biomass and Bioenergy*, [online] Available at: http://www.sciencedirect.com/science/article/pii/S0961953410004307 [Accessed 2 August 2015].

DeCastro, C., Sauvage, E., Valkenberg, M.H. & Hölderich, W.F., 2000. Immobilised Ionic Liquids as Lewis Acid Catalysts for the Alkylation of Aromatic Compounds with Dodecene. *Journal of Catalysis*, [online] Available at: http://www.sciencedirect.com/science/article/pii/S0021951700930045 [Accessed 30 July 2015].

Dimovski, S., 2006. *Structure, characterization and exploration of synthesis of conical and polyhedral crystals of graphite.* 3202891 Ph.D. Drexel University. Available at: http://search.proquest.com/docview/305324532?accountid=50207 [Accessed 31 July 2015].

Gong, J., Liu, J., Jiang, Z., Chen, X., Wen, X., Mijowska, E. & Tang, T., 2014. Converting mixed plastics into mesoporous hollow carbon spheres with controllable diameter. *Applied Catalysis B: Environmental*, [online] Available at: http://www.sciencedirect.com/science/article/pii/S092633731400071X [Accessed 31 July 2015].

IEA, 2014. *Market Energy Investment Outlook*. France: Agency, I.E.

Ioroi, T., Akita, T., Yamazaki, S.-i., Siroma, Z., Fujiwara, N. & Yasuda, K., 2006. Comparative study of carbon-supported Pt/Mo-oxide and PtRu for use as CO-

tolerant anode catalysts. *Electrochimica Acta*, [online] Available at: http://www.sciencedirect.com/science/article/pii/S0013468606006268 [Accessed 30 July 2015].

Islam, A., Taufiq-Yap, Y.H., Chan, E.-S., Moniruzzaman, M., Islam, S. & Nabi, M.N., 2014. Advances in solid-catalytic and non-catalytic technologies for biodiesel production. *Energy Conversion and Management*, [online] Available at: http://www.sciencedirect.com/science/article/pii/S0196890414003410 [Accessed 28 July 2015].

Islam, A., Taufiq-Yap, Y.H., Ravindra, P., Moniruzzaman, M. & Chan, E.-S., 2013. Development of a procedure for spherical alginate–boehmite particle preparation. *Advanced Powder Technology*, [online] Available at: http://www.sciencedirect.com/science/article/pii/S0921883113000769 [Accessed 30 July 2015].

Jakeria, M.R., Fazal, M.A. & Haseeb, A.S.M.A., 2014. Influence of different factors on the stability of biodiesel: A review. *Renewable and Sustainable Energy Reviews*, [online] Available at: http://www.sciencedirect.com/science/article/pii/S1364032113006837 [Accessed 15 July 2015].

Jing, S., Luo, L., Yin, S., Huang, F., Jia, Y., Wei, Y., Sun, Z. & Zhao, Y., 2014. Tungsten nitride decorated carbon nanotubes hybrid as efficient catalyst supports for oxygen reduction reaction. *Applied Catalysis B: Environmental*, [online] Available at: http://www.sciencedirect.com/science/article/pii/S0926337313006516 [Accessed 31 July 2015].

Julkapli, N.M. & Bagheri, S., 2015. Graphene supported heterogeneous catalysts: An overview. *International Journal of Hydrogen Energy*, [online] Available at: http://www.sciencedirect.com/science/article/pii/S0360319914030055 [Accessed 30 July 2015].

Kouzu, M., Yamanaka, S.-y., Hidaka, J.-s. & Tsunomori, M., 2009. Heterogeneous catalysis of calcium oxide used for transesterification of soybean oil with refluxing methanol. *Applied Catalysis A: General*, [online] Available at: http://www.sciencedirect.com/science/article/pii/S0926860X08007540 [Accessed 1 August 2015].

Kuila, U., McCarty, D.K., Derkowski, A., Fischer, T.B., Topór, T. & Prasad, M., 2014. Nano-scale texture and porosity of organic matter and clay minerals in organic-rich mudrocks. *Fuel*, [online] Available at: http://www.sciencedirect.com/science/article/pii/S0016236114006024 [Accessed 30 July 2015].

Lam, M.K., Lee, K.T. & Mohamed, A.R., 2010. Homogeneous, heterogeneous and enzymatic catalysis for transesterification of high free fatty acid oil (waste cooking oil) to biodiesel: a review. *Biotechnol Adv*, [online] Available at: http://www.ncbi.nlm.nih.gov/pubmed/20362044 [Accessed 12 July 2015].

Lee, J.-S. & Saka, S., 2010. Biodiesel production by heterogeneous catalysts and supercritical technologies. *Bioresource Technology*, [online] Available at: http://www.sciencedirect.com/science/article/pii/S0960852410007571 [Accessed 1 August 2015].

Li, Y., Liu, J.H., Witham, C.A., Huang, W., Marcus, M.A., Fakra, S.C., Alayoglu, P., Zhu, Z., Thompson, C.M., Arjun, A., Lee, K., Gross, E., Toste, F.D. & Somorjai, G.A., 2011. A Pt-cluster-based heterogeneous catalyst for homogeneous catalytic reactions: X-ray absorption spectroscopy and reaction kinetic studies of their activity and stability against leaching. *J Am Chem Soc*, [online] Available at: http://www.ncbi.nlm.nih.gov/pubmed/21721543 [Accessed 1 August 2015].

Liaw, K.J., 2013. *Biodiesel Synthesis via Solid acid Catalyst by Using Palm Fatty Acid Distillate (PFAD) as Feedstock.* Degree. Universiti Tunku Abdul Rahman. Available at: http://eprints.utar.edu.my/id/eprint/894 [Accessed 16 July 2013].

López, D.E., Goodwin Jr, J.G., Bruce, D.A. & Lotero, E., 2005. Transesterification of triacetin with methanol on solid acid and base catalysts. *Applied Catalysis A: General*, [online] Available at: http://www.sciencedirect.com/science/article/pii/S0926860X05006186 [Accessed 29 July 2015].

Ma, F. & Hanna, M.A., 1999. Biodiesel production: a review1. *Bioresource Technology*, [online] Available at: http://www.sciencedirect.com/science/article/pii/S0960852499000255 [Accessed 12 July 2015].

Marchetti, J.M., Miguel, V.U. & Errazu, A.F., 2007. Heterogeneous esterification of oil with high amount of free fatty acids. *Fuel*, [online] Available at: http://www.sciencedirect.com/science/article/pii/S0016236106003516 [Accessed 2 August 2015].

Mbaraka, I. & Shanks, B., 2006. Conversion of oils and fats using advanced mesoporous heterogeneous catalysts. *Journal of the American Oil Chemists' Society*, [online] Available at: http://dx.doi.org/10.1007/s11746-006-1179-x [Accessed 1 August 2015].

Melero, J.A., Bautista, L.F., Morales, G., Iglesias, J. & Sánchez-Vázquez, R., 2010. Biodiesel production from crude palm oil using sulfonic acid-modified mesostructured catalysts. *Chemical Engineering Journal*, [online] Available at: http://www.sciencedirect.com/science/article/pii/S1385894709008936 [Accessed 29 July 2015].

Melero, J.A., Bautista, L.F., Morales, G., Iglesias, J. & Sánchez-Vázquez, R., 2015. Acid-catalyzed production of biodiesel over arenesulfonic SBA-15: Insights into the role of water in the reaction network. *Renewable Energy*, [online] Available at: http://www.sciencedirect.com/science/article/pii/S0960148114006545 [Accessed 29 July 2015].

Mo, X., López, D.E., Suwannakarn, K., Liu, Y., Lotero, E., Goodwin Jr, J.G. & Lu, C., 2008. Activation and deactivation characteristics of sulfonated carbon

catalysts. *Journal of Catalysis*, [online] Available at: http://www.sciencedirect.com/science/article/pii/S0021951708000171 [Accessed 1 August 2015].

Mosaddegh, E. & Hassankhani, A., 2014. Preparation and characterization of nano-CaO based on eggshell waste: Novel and green catalytic approach to highly efficient synthesis of pyrano[4,3-b]pyrans. *Chinese Journal of Catalysis*, [online] Available at: http://www.sciencedirect.com/science/article/pii/S1872206712607554 [Accessed 31 July 2015].

Ngamcharussrivichai, C., Totarat, P. & Bunyakiat, K., 2008. Ca and Zn mixed oxide as a heterogeneous base catalyst for transesterification of palm kernel oil. *Applied Catalysis A: General*, [online] Available at: http://www.sciencedirect.com/science/article/pii/S0926860X08001129 [Accessed 1 August 2015].

Olutoye, M.A., Wong, C.P., Chin, L.H. & Hameed, B.H., 2014. Synthesis of FAME from the methanolysis of palm fatty acid distillate using highly active solid oxide acid catalyst. *Fuel Processing Technology*, [online] Available at: http://www.sciencedirect.com/science/article/pii/S0378382014000745 [Accessed 20 July 2015].

Özdemir, E., 2015. Enhanced catalytic activity of Co–B/glassy carbon and Co–B/graphite catalysts for hydrolysis of sodium borohydride. *International Journal of Hydrogen Energy*, [online] Available at: http://www.sciencedirect.com/science/article/pii/S0360319915015840 [Accessed 31 July 2015].

Peng, F., Zhang, L., Wang, H., Lv, P. & Yu, H., 2005. Sulfonated carbon nanotubes as a strong protonic acid catalyst. *Carbon*, [online] Available at: http://www.sciencedirect.com/science/article/pii/S0008622305002265 [Accessed 9 August 2015].

Perego, C. & Villa, P., 1997. Catalyst preparation methods. *Catalysis Today*, [online] Available at: http://www.sciencedirect.com/science/article/pii/S0920586196000557 [Accessed 30 July 2015].

Pham Huu, C., Palhares de Miranda, A.L., Navarro-Delmasure, C., Pham Huu Chanh, A. & Moutier, R., 1987. Comparative study of the biosynthesis of PGE2, PGF2α and TXA2 by different organs of genetically hypertensive (SHR) and obese-hypertensive (SHR-fa/fa) rats. *Prostaglandins, Leukotrienes and Medicine*, [online] Available at: http://www.sciencedirect.com/science/article/pii/0262174687901491 [Accessed 30 August 2015].

Ramos-Sánchez, G. & Balbuena, P.B., 2014. CO adsorption on Pt clusters supported on graphite. *Journal of Electroanalytical Chemistry*, [online] Available at: http://www.sciencedirect.com/science/article/pii/S1572665713004323 [Accessed 31 July 2015].

Ramulifho, T., Ozoemena, K.I., Modibedi, R.M., Jafta, C.J. & Mathe, M.K., 2012. Fast microwave-assisted solvothermal synthesis of metal nanoparticles (Pd, Ni, Sn) supported on sulfonated MWCNTs: Pd-based bimetallic catalysts for ethanol oxidation in alkaline medium. *Electrochimica Acta*, [online] Available at: http://www.sciencedirect.com/science/article/pii/S0013468611016239 [Accessed 9 August 2015].

Rattanaphra, D., Harvey, A.P., Thanapimmetha, A. & Srinophakun, P., 2012. Simultaneous transesterification and esterification for biodiesel production with and without a sulphated zirconia catalyst. *Fuel*, [online] Available at: http://www.sciencedirect.com/science/article/pii/S0016236112000567 [Accessed 29 July 2015].

Rexhäuser, S. & Löschel, A., 2015. Invention in energy technologies: Comparing energy efficiency and renewable energy inventions at the firm level. *Energy Policy*, [online] Available at: http://www.sciencedirect.com/science/article/pii/S030142151500066X [Accessed 11 July 2015].

Salavati-Niasari, M., Mirsattari, S.N. & Bazarganipour, M., 2008. Synthesis, characterization and catalytic oxyfunctionalization of cyclohexene with tert-butylhydroperoxide over a manganese(II) complex covalently anchored to multi-wall carbon nanotubes (MWNTs). *Polyhedron*, [online] Available at: http://www.sciencedirect.com/science/article/pii/S0277538708004555 [Accessed 1 August 2015].

Shen, Y., Zhao, P., Shao, Q., Takahashi, F. & Yoshikawa, K., 2014. In situ catalytic conversion of tar using rice husk char/ash supported nickel–iron catalysts for biomass pyrolytic gasification combined with the mixing-simulation in fluidized-bed gasifier. *Applied Energy*, [online] Available at: http://www.sciencedirect.com/science/article/pii/S0306261914011246 [Accessed 31 July 2015].

Shu, Q., Gao, J., Nawaz, Z., Liao, Y., Wang, D. & Wang, J., 2010. Synthesis of biodiesel from waste vegetable oil with large amounts of free fatty acids using a carbon-based solid acid catalyst. *Applied Energy*, [online] Available at: http://www.sciencedirect.com/science/article/pii/S0306261910000887 [Accessed 29 July 2015].

Shu, Q., Zhang, Q., Xu, G. & Wang, J., 2009. Preparation of biodiesel using s-MWCNT catalysts and the coupling of reaction and separation. *Food and Bioproducts Processing*, [online] Available at: http://www.sciencedirect.com/science/article/pii/S0960308509000406 [Accessed 2 August 2015].

Shuit, S. & Tan, S., 2015. Biodiesel Production via Esterification of Palm Fatty Acid Distillate Using Sulphonated Multi-walled Carbon Nanotubes as a Solid Acid Catalyst: Process Study, Catalyst Reusability and Kinetic Study. *BioEnergy Research*, [online] Available at: http://dx.doi.org/10.1007/s12155-014-9545-2 [Accessed 20 July 2015].

Shuit, S.H., Lee, K.T., Kamaruddin, A.H. & Yusup, S., 2010. Reactive extraction and in situ esterification of Jatropha curcas L. seeds for the production of biodiesel. *Fuel*, [online] Available at: http://www.sciencedirect.com/science/article/pii/S001623610900341X [Accessed 9 August 2015].

Shuit, S.H., Ong, Y.T., Lee, K.T., Subhash, B. & Tan, S.H., 2012. Membrane technology as a promising alternative in biodiesel production: A review. *Biotechnology Advances*, [online] Available at: http://www.sciencedirect.com/science/article/pii/S0734975012000468 [Accessed 2 August 2015].

Shuit, S.H. & Tan, S.H., 2014. Feasibility study of various sulphonation methods for transforming carbon nanotubes into catalysts for the esterification of palm fatty acid distillate. *Energy Conversion and Management*, [online] Available at: http://www.sciencedirect.com/science/article/pii/S019689041400079X [Accessed 19 July 2015].

Shuit, S.H., Yee, K.F., Lee, K.T., Subhash, B. & Tan, S.H., 2013. Evolution towards the utilisation of functionalised carbon nanotubes as a new generation catalyst support in biodiesel production: an overview. *RSC Advances*, [online] Available at: http://dx.doi.org/10.1039/C3RA22945A [Accessed 21 July 2015].

Sun, Z.-P., Zhang, X.-G., Liang, Y.-Y. & Li, H.-L., 2009. A facile approach towards sulfonate functionalization of multi-walled carbon nanotubes as Pd catalyst support for ethylene glycol electro-oxidation. *Journal of Power Sources*, [online] Available at: http://www.sciencedirect.com/science/article/pii/S0378775309001918 [Accessed 9 August 2015].

Tay, K.S., 2012. *A Study of Enzymatic Reaction in Biodiesel Conversion Using Fresh and Waste Cooking Oil*. Degree. Universiti Tunku Abdul Rahman. Available at: http://eprints.utar.edu.my/id/eprint/635 [Accessed 16 July 2015].

Tyson, K.S., 2005. DOE analysis of fuels and coproducts from lipids. *Fuel Processing Technology*, [online] Available at: http://www.sciencedirect.com/science/article/pii/S0378382004001948 [Accessed 27 July 2015].

Villa, A., Tessonnier, J.-P., Majoulet, O., Su, D.S. & Schlögl, R., 2010a. Transesterification of Triglycerides Using Nitrogen-Functionalized Carbon Nanotubes. *ChemSusChem*, [online] Available at: http://dx.doi.org/10.1002/cssc.200900181 [Accessed 2 August 2015].

Villa, A., Tessonnier, J.P., Majoulet, O., Su, D.S. & Schlogl, R., 2010b. Transesterification of triglycerides using nitrogen-functionalized carbon nanotubes. *ChemSusChem*, [online] Available at: http://www.ncbi.nlm.nih.gov/pubmed/19908273 [Accessed 9 August 2015].

Wang, L., Han, Q., Li, D., Wang, Z., Chen, J., Chen, S., Zhang, P., Liu, B., Wen, M. & Xu, J., 2013. Comparisons of Pt catalysts supported on active carbon, carbon

molecular sieve, carbon nanotubes and graphite for HI decomposition at different temperature. *International Journal of Hydrogen Energy*, [online] Available at: http://www.sciencedirect.com/science/article/pii/S0360319912023403 [Accessed 31 July 2015].

Wang, Y., Ou, S., Liu, P., Xue, F. & Tang, S., 2006. Comparison of two different processes to synthesize biodiesel by waste cooking oil. *Journal of Molecular Catalysis A: Chemical*, [online] Available at: http://www.sciencedirect.com/science/article/pii/S1381116906005772 [Accessed 29 July 2015].

Wang, Z.-B., Yin, G.-P. & Lin, Y.-G., 2007. Synthesis and characterization of PtRuMo/C nanoparticle electrocatalyst for direct ethanol fuel cell. *Journal of Power Sources*, [online] Available at: http://www.sciencedirect.com/science/article/pii/S0378775307007458 [Accessed 30 July 2015].

Warabi, Y., Kusdiana, D. & Saka, S., 2004. Reactivity of triglycerides and fatty acids of rapeseed oil in supercritical alcohols. *Bioresource Technology*, [online] Available at: http://www.sciencedirect.com/science/article/pii/S0960852403002025 [Accessed 29 July 2015].

Wu, B., Kuang, Y., Zhang, X. & Chen, J., 2011. Noble metal nanoparticles/carbon nanotubes nanohybrids: Synthesis and applications. *Nano Today*, [online] Available at: http://www.sciencedirect.com/science/article/pii/S1748013210001696 [Accessed 30 July 2015].

Yujaroen, D., Goto, M., Sasaki, M. & Shotipruk, A., 2009. Esterification of palm fatty acid distillate (PFAD) in supercritical methanol: Effect of hydrolysis on reaction reactivity. *Fuel*, [online] Available at: http://www.sciencedirect.com/science/article/pii/S0016236109001203 [Accessed 25 July 2015].

Zabeti, M., Daud, W.M.A.W. & Aroua, M.K., 2009a. Optimization of the activity of CaO/Al2O3 catalyst for biodiesel production using response surface methodology. *Applied Catalysis A: General*, [online] Available at: http://www.sciencedirect.com/science/article/pii/S0926860X09004840 [Accessed 1 August 2015].

Zabeti, M., Wan Daud, W.M.A. & Aroua, M.K., 2009b. Activity of solid catalysts for biodiesel production: A review. *Fuel Processing Technology*, [online] Available at: http://www.sciencedirect.com/science/article/pii/S0378382009000629 [Accessed 12 July 2015].

Zhang, Y., Dubé, M.A., McLean, D.D. & Kates, M., 2003. Biodiesel production from waste cooking oil: 1. Process design and technological assessment. *Bioresource Technology*, [online] Available at:

http://www.sciencedirect.com/science/article/pii/S0960852403000403 [Accessed 23 July 2015].

Zong, M.-H., Duan, Z.-Q., Lou, W.-Y., Smith, T.J. & Wu, H., 2007. Preparation of a sugar catalyst and its use for highly efficient production of biodiesel. *Green Chemistry*, [online] Available at: http://dx.doi.org/10.1039/B615447F [Accessed 1 August 2015].

APPENDICES

APPENDIX A: Detailed Data and Graphs Generated by XRD

APPENDIX B: FTIR Spectra of Original, Purified and Sulfonated Graphite Catalysts

APPENDIX C: Results of Gas Chromatography

APPENDIX D: MSDS of All Chemicals Used